

ABSTRACTS



Centre of Excellence: *Magnetic and Molecular Materials for Future Electronics*

Institute of Molecular Physics, Polish Academy of Sciences
ul. Mariana Smoluchowskiego 17, 60-179 Poznań, Poland

THE MAGNETISM OF ULTRATHIN TRILAYERS: A PLAYGROUND TO STUDY FUNDAMENTALS

K. Baberschke

Institut fuer Experimentalphysik, Freie Universitaet Berlin, Berlin, Germany

Ferromagnets of few atomic layers only allow to manipulate magnetism as it is not accessible in 3D bulk. Special growth of ultrathin films produces artificial crystallographic structures like tetragonal Ni for which changes of $\approx 0.05\text{\AA}$ in the geometry enlarge the magnetic anisotropy by $10^2 - 10^3$. For Fe, Co, Ni the Curie-temperatures can be adjusted by varying the number of layers to any value between zero and T_C^{bulk} . In particular we focus on experiments in coupled FM films like Co/Cu/Ni. X-ray magnetic circular dichroism (XMCD) enables us to measure separately T_C^{Ni} and T_C^{Co} . They influence each other dramatically due to enhanced spin fluctuations in 2D [1]. This is a case study which cannot be explained in a mean-field approach of $\langle S_z \rangle$ but needs higher order contributions of spin dynamics by S^2 . With ferromagnetic resonance (FMR) of coupled trilayers we monitor the optical and acoustical modes of the spin waves and determine the interlayer exchange coupling, its strength (eV/particle) and its temperature dependence [2]. From the linewidth we show conclusively that ‘non *Gilbert*-like’ damping at interfaces of nanostructures may be dominant. Finally, we discuss the alignment of orbital and spin moment at interfaces, i.e. the breakdown of the third Hund’s rule [2].

Supported in part by DFG, Sfb 290 and BMBF (05KS1 KEB4).

[1] K. Baberschke and P. Pouloupoulos in *Band-Ferromagnetism*, edited by K. Baberschke, M. Donath, W. Nolting (Springer, Berlin 2001), p. 27 and p. 283

[2] J. Lindner et al., Phys. Rev. Lett. **88**, 167206 (2002);

F. Wilhelm et al., Phys. Rev. Lett. **87**, 207202 (2001)



Centre of Excellence: Magnetic and Molecular Materials for Future Electronics

Institute of Molecular Physics, Polish Academy of Sciences
ul. Mariana Smoluchowskiego 17, 60-179 Poznań, Poland

MAGNETISM UNDER THE SCANNING TUNNELING MICROSCOPE

S. Heinze¹, D. Wortmann², G. Bihlmayer², and S. Bluegel²

¹ Institute of Applied Physics, University of Hamburg, D-20355 Hamburg, Germany

² Institut fuer Festkoerperforschung, Forschungszentrum Juelich, D-52425 Juelich, Germany

At surfaces one experiences magnetic structures on a wide range of different length scales. These include the microscopic length scale at which magnetic domains form, or mesoscopic length scale determined by nano-patterning or the natural occurrence of steps at surfaces and then the atomic length scale of clusters, wires and atomic scale magnetic structures such as for example the antiferromagnetic structure. In this frontier field of nanomagnetism observing and understanding complex magnetic structures is crucial. In the recent years the spin-polarized scanning tunneling microscope (SP-STM) developed to a tool to unravel complex magnetic superstructures on different length scales. For setting a frame of reference, in this lecture we will first present a list of results for atomic scale magnetic structures, give some explanation how to understand those and then we will move to the discussion of the spin-polarized scanning tunneling microscope. We will extend the model of Tersoff and Hamann to the situation of an STM with a spin-polarized tip with an arbitrary magnetization direction and a sample with an arbitrary magnetic structure and discuss the different operation modes of a SP-STM: We show that the spectroscopy mode (SP-STs) is ideal to analyse complex magnetic structures on a mesoscopic length scale created by atomic-scale ferromagnetism and we propose the application of the constant current mode of a SP-STM to the investigation of surfaces of complex atomic-scale magnetic structures of otherwise chemically equivalent atoms. We will discuss several examples. The results presented are obtained within the standard-model for describing magnetic transition metals, which is the density functional theory. The results are obtained with the full-potential linearized augmented plane wave method in the vector-spin density formulation to treat complex non-collinear magnetic structures in low-dimensional systems.



Centre of Excellence: Magnetic and Molecular Materials for Future Electronics

Institute of Molecular Physics, Polish Academy of Sciences
ul. Mariana Smoluchowskiego 17, 60-179 Poznań, Poland

**MAGNETIC AND SPECTROSCOPIC PROPERTIES OF FREE AND SUPPORTED
TRANSITION METAL CLUSTERS**

H. Ebert

Department Chemistry / Physical Chemistry
University of Munich, Germany

Magnetic clusters receive recently a lot of attention in academic but also in technological research. On the one hand side, the interest is caused by the fact that clusters provide a bridge between atoms and bulk material often showing quite peculiar properties. On the other hand, the ongoing need for miniaturizing, in particular in data storage technology, leads to smaller and smaller functional units leading finally to small clusters. The lecture will give an overview on the activities in this rapidly growing field, including free transition metal clusters, that can be seen as reference systems. While a number of experimental results will be presented and discussed in the first part of the lecture, emphasize will be put on concepts and results of theoretical investigations. In particular, it will be demonstrated that theory is able to provide very important and helpful information to understand the various properties of magnetic clusters that in general strongly depend on their composition, size and shape. This applies especially if one considers properties that are caused by spin-orbit coupling as the magnetic anisotropy. Another example is the linear and circular magnetic dichroism showing up in electron spectroscopies that are for that reason very powerful tools to investigate the properties of magnetic clusters.



Centre of Excellence: Magnetic and Molecular Materials for Future Electronics

Institute of Molecular Physics, Polish Academy of Sciences
ul. Mariana Smoluchowskiego 17, 60-179 Poznań, Poland

ELECTRONIC STRUCTURE OF DILUTE MAGNETIC SEMICONDUCTORS

Olle Eriksson,
Uppsala University

A brief background to the technological implications of dilute magnetic semiconductors is given after which several materials related issues are discussed for this class of compounds. The focus of the talk will be on electronic structure related phenomena, such as magnetic ordering, critical temperatures and defect formation energies. In addition to commonly discussed dilute magnetic semiconductors (e.g. Mn doped GaAs) several novel materials will be discussed, e.g. Co-oxides that recently have been predicted from first principles theory to be ferromagnetic semiconductors. The results of a newly developed theory for transport properties on magnetic nano-structures will be discussed with focus on spin-filtering applications.



Centre of Excellence: Magnetic and Molecular Materials for Future Electronics

Institute of Molecular Physics, Polish Academy of Sciences
ul. Mariana Smoluchowskiego 17, 60-179 Poznań, Poland

RELATIVISTIC DENSITY FUNCTIONAL APPROACH AND MAGNETISM

H. Eschrig, M. Richter and I. Ophale

IFW Dresden, P.O.Box 27 01 16, D-01171 Dresden, Germany

The derivation of Kohn-Sham-Dirac types of equations is revisited and a number of subtleties is focussed on, including several accuracy issues. A survey over typical relativistic effects in the electronic structure of solids as on the symmetry of the states, effects on valence, binding and on optical properties is given. The interplay of spin-orbit coupling and correlation in the formation of the magnetic ground state of solids without and with an applied magnetic fields is considered in some more detail.

An extended version of the presented material including computational details will appear in: H. Eschrig, M. Richter and I. Ophale, Relativistic Solid State Calculations, in: *Relativistic Electronic Structure Theory-Part II: Applications*, edited by P. Schwerdtfeger, Elsevier, Amsterdam, 2003, Chap. 12.



Centre of Excellence: Magnetic and Molecular Materials for Future Electronics

Institute of Molecular Physics, Polish Academy of Sciences
ul. Mariana Smoluchowskiego 17, 60-179 Poznań, Poland

AB-INITIO CALCULATIONS FOR LOW-DIMENSIONAL MAGNETIC SYSTEMS

Volker Eyert

Institut für Physik, Universität Augsburg

Low-dimensional physical systems keep on receiving a lot of attention due to the occurrence of fascinating behaviour deviating distinctly from the notions connected with the three-dimensional world. In particular, materials with reduced dimensionality may exhibit new kinds of excitations such as spinons and holons as well as ordering phenomena as, e.g., Peierls transitions and charge density waves. Further interest grows out of the deviations from strict one- or two-dimensionality as arising from interactions between the low-dimensional units. They lead to a range of different coupling strengths and may increase the spectrum of low-temperature phases.

Magnetic systems are no exception in this respect but bear the additional attraction of being subject to the Mermin-Wagner theorem, which prohibits long-range magnetic order at finite temperatures for one- and two-dimensional arrangements of localized magnetic moments. On the experimental side this has motivated the preparation and characterization of magnetic layer materials, chain compounds or spin-ladder systems with localized moments arising from unfilled transition metal or f-electron atoms. Theoretically such compounds have been investigated using first principles methods, model approaches or combinations of both aiming particularly at an understanding of the coupling mechanisms as well as the long-range ordering of the magnetic moments.

In the talk I will illustrate the magnetic properties of low-dimensional systems by considering, in particular, magnetic chain compounds using first principles methods as based on density functional theory. After a short account of the capabilities offered by first principles methods I will discuss the electronic and magnetic properties of a rather new class of magnetic chain compounds, a prototype being the cobaltate $\text{Ca}_3\text{Co}_2\text{O}_6$. All members of this class are characterized by strong interactions between the magnetic ions of each chain across non-magnetic transition-metal atoms. In contrast, the magnetic coupling between different chains is very weak. Forming a triangular lattice, antiferromagnetic interchain coupling as displayed by some of these compounds may give rise to interesting frustration effects and a broad range of different magnetic structures.



Centre of Excellence: Magnetic and Molecular Materials for Future Electronics

Institute of Molecular Physics, Polish Academy of Sciences

ul. Mariana Smoluchowskiego 17, 60-179 Poznań, Poland

**NANOCRYSTALLINE ALLOYS:
STRUCTURAL ASPECTS AND MAGNETIC PROPERTIES**

J.-M. Greneche

Laboratoire de Physique de l'Etat Condensé , UMR CNRS 6087 Université du Maine,
72085 Le Mans Cedex 9, France
e-mail : greneche@univ-lemans.fr

Nanocrystalline alloys as Finemet, Nanoperm, and Hitperm, are fascinating systems because of their two phase behaviour. Their structural properties can be thus described by the emergence of crystalline grains in a residual amorphous matrix when a subsequent annealing treatment is applied to the as-quenched precursor alloy. The proportions of those two components are strongly dependent on the annealing temperature but less dependent on the annealing time. Both the structural and magnetic characterization of the nanocrystalline alloys requires the use of different techniques. A large debate occurred during the last ten years.

During the presentation, a few words will be first devoted to the preparation of those materials and the thermodynamical aspects. Then we concentrate on the structural characterization of both the crystalline grains and the amorphous residual phase, as well as the nature and the role of the interfacial zone which is located between these two components. Then, we discuss the magnetic properties from a macroscopic point of view and also from a local point of view, in order to clarify some concepts and to discuss the role of the amorphous remainder and the intergranular phase on the magnetic properties, as a function of the crystalline fraction.

Finally, some perspectives of applications will be reported after reviewing the magnetic performances of the nanocrystalline alloys, in comparison with usual materials.



FIRST-PRINCIPLES INVESTIGATIONS OF MAGNETIC NANOSTRUCTURES

Juergen Hafner and Daniel Spisak

Institut fuer Materialphysik and Center for Computational Materials Science,
Universitaet Wien, A-1090 WIEN, Austria

The physics of magnetic nanostructures is of great scientific and technological interest: the magnetic properties of nanostructures are found to be very often drastically different from those of the bulk material, they vary with the dimensionality and the size of the nanostructures. The structural and magnetic characterization of nanostructures in the laboratory turns out to be difficult and almost necessarily incomplete. E.g., the total magnetization of a thin film can be measured using magnetic X-ray circular dichroism (MXCD), but layer-resolved information on the magnetic structure of the film is not available. Under these circumstances, theoretical modelling with a predictive capacity is of particular importance.

Ab-initio local-spin-density theory has proved to be an immensely valuable tool for the investigation of the energetics and the geometric, electronic and magnetic properties of nanostructures. In my lecture I shall very briefly outline the foundations of the approach and the capacities and limitations of modern density-functional codes. Applications to nanostructures from 0 to 2 dimensions will be reviewed:

- (i) Structural and magnetic properties of metallic clusters, including noncollinear structures.
- (ii) Nanowires and nanostripes: Fe-nanowires on stepped Cu-templates, magnetism in nanowires formed by 4d- and 5d-transition metals, striped Fe-phases on reconstructed Ir-surfaces.
- (iii) Ultrathin films. Particular attention will be devoted to the correlation between structure and magnetism of ultrathin Fe-films on Cu(100) and Cu(111) films and their correlation with the magnetic properties of alpha- and gamma-Fe.



Centre of Excellence: Magnetic and Molecular Materials for Future Electronics

Institute of Molecular Physics, Polish Academy of Sciences
ul. Mariana Smoluchowskiego 17, 60-179 Poznań, Poland

NONCOLLINEAR MAGNETISM AND PHASE-STABILITY OF MN

Juergen Hafner and Daniel Spisak

Institut fuer Materialphysik and Center for Computational Materials Science,
Universitaet Wien, A-1090 WIEN, Austria

Manganese is probably (except perhaps plutonium) the most complex of all metallic elements. At ambient pressure and low temperatures, the stable phase, alpha-Mn, has a complex body-centred cubic structure with 29 atoms in the primitive cell. At higher temperatures, Mn undergoes successively structural transformations to a simple cubic (beta-Mn), a face-centred-cubic (gamma-Mn) and a body-centred-cubic (delta-Mn). Under pressure, Mn transforms to a fifth phase which has been tentively described as close-packed hexagonal (epsilon-Mn). Below a Neel temperature of $T_N=95$ K, alpha-Mn transforms to a complex noncollinear antiferromagnetic structure. The magnetic transition is coupled to a tetragonal distortion of the crystal structure. Beta-Mn has been characterized as a spin-liquid, geometric frustration suppresses magnetic ordering down to the lowest temperatures. The remaining three polymorphs also show complex low-spin/high-spin transitions. So far, the explanation of the complex structural and magnetic phase diagram of Mn remained a massive challenge to theory. In this lecture, a first-principles local-spin-density investigation of noncollinear magnetism and phase stability in Mn will be presented.



Centre of Excellence: Magnetic and Molecular Materials for Future Electronics

Institute of Molecular Physics, Polish Academy of Sciences
ul. Mariana Smoluchowskiego 17, 60-179 Poznań, Poland

**TRANSPORT AND MAGNETIC PROPERTIES OF
FERROMAGNETIC (III, MN)V SEMICONDUCTORS**

T. Jungwirth

Institute of Physics, Academy of Sciences of the Czech Republic, Prague, Czech Republic

The basic microscopic origins of ferromagnetism in the (III,Mn)As and (III,Mn)Sb compounds appear to be well understood within a model of carrier induced magnetic interactions between Mn local moments. Efficient computation methods have been developed, based on the effective Hamiltonian description of the system, which are able to model their magnetic, transport, and optical properties on a semi-quantitative level. In this presentation we focus on the ferromagnetic transition temperature and remanent magnetization, and discuss also the comparison between theory and experiment for the anisotropic magnetoresistance effects and the anomalous Hall effect. We also discuss a microscopic theory of the Gilbert damping of magnetization precession and the spin-transfer process in diluted magnetic semiconductor heterostructures.



Centre of Excellence: Magnetic and Molecular Materials for Future Electronics

Institute of Molecular Physics, Polish Academy of Sciences
ul. Mariana Smoluchowskiego 17, 60-179 Poznań, Poland

RECENT DEVELOPMENTS IN NANOSCALE MAGNETISM

J. Kirschner *

Max-Planck-Institut fuer Mikrostrukturphysik
Weinberg 2
06120 Halle

An actual field of research in magnetism is the analysis of nanostructures. I will report on two lines of development aiming at spatial analysis of nanostructures and at the dynamics of collective excitations at small wavelengths, down to the unit cell at surfaces.

Spatial analysis may be obtained by spin-polarized tunneling spectroscopy, if a suitable electronic structure of tip or sample is available. We introduced a more general approach which probes the spin-dependent density of states in the sample, leading to a change in tunneling current upon reversing the tip magnetization. While our previous development was confined to perpendicularly magnetized structures in the sample, we are now able to probe in-plane magnetized domains. This is achieved by using a tip on a disk-shaped electrode which is magnetized along the sample surface. Examples for both approaches are given.

The quest for the study of short-wavelength magnetic surface excitations has been long-standing. We report on the development of spin-polarized electron energy loss spectroscopy, by means of which the dispersion relation of surface magnons may be mapped up to the zone boundary. First examples for Co films on Cu(100) are given.

*** work done in collaboration with W. Wulfhekel, H. F. Ding, U. Schlickum, R. Vollmer, H. Ibach, A. Kumar, and M. Etzkorn**



Centre of Excellence: Magnetic and Molecular Materials for Future Electronics

**Institute of Molecular Physics, Polish Academy of Sciences
ul. Mariana Smoluchowskiego 17, 60-179 Poznań, Poland**

**NONLINEAR TRANSPORT OF ELECTRONS AND SPINS IN
CORRELATED MESOSCOPIC STRUCTURES**

H. Kroha

Physikalisches Institut der Universitaet Bonn, Bonn, Germany

In nanoscopic quantum dots the strong charging energy can induce a local magnetic moment on the dot, and due to the coupling to the leads can lead to dynamical electron and spin correlations, in particular the Kondo effect. Since spectroscopy as well as transport on such systems require in general a finite bias voltage, it is necessary to describe such correlated systems in a nonequilibrium situation. We describe a newly developed poor mans scaling renormalization group method for Kondo systems at finite bias voltage. Several applications will then be discussed in detail, namely the nonequilibrium quasiparticle distribution in quantum wires with Kondo impurities, including its relevance for the low-temperature dephasing problem and the use of quatum dots in a local magnetic fields as spin filters.



Centre of Excellence: Magnetic and Molecular Materials for Future Electronics

Institute of Molecular Physics, Polish Academy of Sciences
ul. Mariana Smoluchowskiego 17, 60-179 Poznań, Poland

HEAVY-FERMION SYSTEMS AT A MAGNETIC INSTABILITY

H. v. Loehneysen

*Physikalisches Institut, Universitaet Karlsruhe, D-76128 Karlsruhe, Germany and
Forschungszentrum Karlsruhe, Institut fuer Festkoerperphysik, D-76021 Karlsruhe, Germany*

The groundstate of a number of metals, notably those with strong electronic correlations such as heavy fermion systems or weak itinerant magnets, is in close proximity to a magnetic instability. The transition from a Pauli-paramagnetic to a magnetically ordered state can be tuned by chemical composition, pressure, or magnetic field. Often pronounced deviations from Fermi-liquid behavior are observed in the vicinity of the quantum critical point (QCP) where the magnetic ordering temperature vanishes, which are commonly referred to as non-Fermi-liquid (NFL) behavior.

The scenario of incipient magnetic order is exemplified by CeCu₆ with a nonmagnetic groundstate, and long-range incommensurate antiferromagnetism in CeCu_{6-x}Au_x for $x > x_c = 0.1$. The magnetic instability can be tuned by alloying or applying external pressure p . At the QCP, the specific heat C varies as $C/T \sim \ln(T/T_0)$, independent of whether the Néel temperature T_N is tuned to zero by variation of x or p , and one observes a linear resistivity contribution $\Delta\rho \sim T$ [1]. These NFL features can be explained by quasi two-dimensional critical fluctuations, as observed for $x = 0.1$ with inelastic neutron scattering [2]. In addition, unusual dynamic scaling laws for the dynamical susceptibility are found in the vicinity of the QCP in CeCu_{6-x}Au_x which are incompatible with simple spin-fluctuation scenarios [3].

A particularly clean system where the magnetic order – a long-wavelength incommensurate structure – can be tuned to $T = 0$ by hydrostatic pressure is MnSi. Here an unusual $T^{1.5}$ dependence of the electrical resistivity is observed far beyond the critical pressure [4]. Recent elastic neutron scattering indicate that near the QCP the system becomes orientationally disordered, with some resemblance of liquid crystals [5].

The archetypal weak ferromagnet ZrZn₂ has long been considered a candidate for p-wave superconductivity if samples can be made sufficiently pure. We recently found evidence for superconductivity in ZrZn₂ single crystals of unprecedented purity [6]. Surprisingly, superconductivity (with $T_c \approx 0.3$ K) exists over the entire pressure range where ferromagnetism exists, and vanishes when ferromagnetism is suppressed at sufficiently high pressure.

- [1] H. v. Loehneysen, J. Phys.: Cond. Matt. **8** (1996) 9689-9706
- [2] O. Stockert et al., Phys. Rev. Lett. **80** (1998) 5627-5630
- [3] A. Schroeder et al., Nature **407** (2000) 351-355
- [4] C. Pfleiderer et al., Nature **414** (2001) 427-431
- [5] C. Pfleiderer et al., to be published
- [6] C. Pfleiderer et al., Nature **412** (2001) 58-61



MAGNETISM IN LOW-DIMENSIONAL CUPRATES

K.-H. Mueller

IFW Dresden, POB 270116, D-01171 Dresden, Germany

The interest in quasi low-dimensional cuprates originated from the discovery of high- T_c superconductors typically consisting of intermediate valence ("doped") copper oxide planes with strongly correlated d -electrons. For understanding the mechanism of superconductivity in these materials their magnetic properties, even in the non-doped state, have to be considered. The magnetism of the cuprates mainly originates from the d -electrons of copper in the oxidation states Cu^I , Cu^{II} or Cu^{III} . In an ionic approximation the Cu species are described by charge states, e.g. Cu^{II} by Cu^{2+} . According to this approximation the ground state of Cu^I compounds has no magnetic moment and they exhibit diamagnetism or *van Vleck* paramagnetism. Cu^{2+} has an odd number of d -electrons resulting in so called *Kramers* degeneracy. Its paramagnetic moment is well approximated by the spin-only value of 1.73 Bohr magnetons. Depending on its anionic surrounding the paramagnetic moment of Cu^{3+} corresponds to the high-spin value of 2.83 Bohr magnetons (as in K_3CuF_6) or it may be zero (low spin) as usually in cuprates. In the ionic approximation a certain overlap of wave functions results in exchange interactions of the magnetic moments which may lead to antiferromagnetic or ferromagnetic long-range order. In the case of cuprates the dominating type of interaction is superexchange via oxygen anions. In a more realistic description covalence or, more generally, overlapping electron-wave functions combined with electron correlation have to be taken into account in order to explain effects as (i) the existence of well localized magnetic moments (in spite of delocalized wave functions), (ii) the real electric charge of the species usually being much smaller than following from the formal valency, (iii) the metallic or insulating behavior of particular compounds as e.g. LaCuO_3 or La_2CuO_4 , respectively, and (iv) the special crystallographic structures which in the case of Cu^I compounds usually contain O-Cu-O dumbbells. In most cases the Cu^{II} cuprates contain quasi two-dimensional or quasi one-dimensional networks of CuO_4 plaquettes and they mostly behave like quantum spin-1/2 antiferromagnets of low dimensionality ($d = 1$ or $d = 2$). Usually a crossover to three-dimensional behavior occurs in these compounds at sufficiently low temperatures because, actually, they are three-dimensional solids. Ladder compounds are



Centre of Excellence: Magnetic and Molecular Materials for Future Electronics

Institute of Molecular Physics, Polish Academy of Sciences
ul. Mariana Smoluchowskiego 17, 60-179 Poznań, Poland

a special interesting group of cuprates. In the ideal case where non-interacting ladders have antiferromagnetic interactions between spin-1/2 sites, with the same strength of the interaction along the rungs and the legs, two types of behavior can be distinguished. Even-leg-ladder compounds reveal a spin gap, resulting in an exponentially vanishing magnetic susceptibility χ whereas in the odd-leg-ladder compounds χ remains finite for temperature $T \rightarrow 0$. This simple picture becomes more complicated if there are deviations from the ideal cases. In particular phenomena have been observed which can be attributed to crossovers between effective dimensionalities of $d = 0, 1, 2$, and 3 .



**UNCONSTRAINED NON-COLLINEAR CALCULATIONS OF COMPLEX
MAGNETIC MATERIALS**

L. Nordstroem

Department of Physics, Uppsala University, Uppsala, Sweden

A short review of spin-dependent density functional theory will be given followed by a historic account of the development within applications: collinear, atomic moment based non-collinear, and fully unconstrained non-collinear. After a description of how this can be implemented in a full potential electronic structure method, some examples of applications will be given. These will touch upon e.g. relativistic effects, spin density waves, and spin waves.



Centre of Excellence: Magnetic and Molecular Materials for Future Electronics

Institute of Molecular Physics, Polish Academy of Sciences
ul. Mariana Smoluchowskiego 17, 60-179 Poznań, Poland

MAGNETIC TUNNEL JUNCTIONS
REVIEW OF EXPERIMENTAL RESULTS AND PERSPECTIVES

F. Petroff

Unité Mixte de Physique CNRS/Thales, Domaine de Corbeville, 91404 Orsay, France

and

Université Paris-Sud, 91405 Orsay, France

Stimulated by the discovery of the Giant Magnetoresistance effect¹ in 1988, spin electronics or spintronics has developed into one of the most vigorous field of research in condensed matter physics. One of the areas of considerable interest concerns the research on magnetic tunnel junctions and the associated Spin Dependent Tunneling (SDT) effect reported for the first time at room temperature in 1995 by Moodera et al². Within a few years, the understanding of the fundamental physics underlying SDT has considerably evolved while important advances towards applications such as magnetic random-access memories were made.

After a general introduction on magnetic tunnel junctions, I will review some of the recent experiments performed to identify the relevant parameters driving the SDT effect and discuss its current understanding. Some perspectives and new directions for further research will be discussed at the end of the lecture.

¹ *M.N. Baibich et al, Phys. Rev. Lett. 61, 2472 (1988)*

² *J.S. Moodera et al, Phys. Rev. Lett. 74, 3273 (1995)*



**ELECTRONIC STRUCTURE AND THERMODYNAMICAL PROPERTIES OF
SOME TERNARY d AND f ELECTRON INTERMETALLICS**

A. Ślebarski

Institute of Physics, University of Silesia, 40-007 Katowice

A. Jezierski

Institute of Molecular Physics, Polish Academy of Sciences, 60-179 Poznań

CeNiSn and CeRhSb exhibit an puzzled ground state in the Kondo lattice. The class of these materials, e.g., "Kondo insulators", is characterized by their electronic properties, which at high temperatures is associated with a set of independent localized 4f moments interacting with the conduction electrons, while at low temperatures the electronic properties resemble those of narrow gap of the order ~ 10 K. The energy gap is due to the hybridization between the strongly correlated 4f electrons and a conduction band, which is almost half filled.

The compounds CeNiSn and CeRhSb are only two in the equiatomic ternary series which show a hybridization gap in the electronic density of states at low temperatures and a paramagnetic ground state. While the Ce-based ternary Sn-compounds are antiferromagnetically ordered (e.g., CeCuSn, CeAgSn, CePdSn) the equiatomic antimonides CeMSb (M=Ni, Pd, Pt) are ferromagnets. Recently we have discovered, that the electrical resistivity, magnetic susceptibility and specific heat measurements of CeRhSn have power law with low exponents, characteristic of a non-Fermi liquid ground state.

The main goal of this presentation is to find the influence of transition metal M on the coherent gap formation at the Fermi level.

We also discuss a similar semiconductor-like resistance anomaly of Fe₂TiSn. Fe₂TiSn reveal the occurrence of weak ferromagnetism and heavy fermion-like behavior. A similar feature in the electronic structure and semiconductor-like resistance anomaly have been observed in FeSi and CeNiSn, which both are classified as Kondo insulators.



SIC-LSD DESCRIPTION OF HALF-METALLIC TRANSITION METAL OXIDES

Z. Szotek¹, W.M. Temmerman¹, D. Koedderitzsch², A. Svane³, L. Petit³, G.M. Stocks⁴,
W. Hergert², and H. Winter⁵

¹ Daresbury Laboratory, Daresbury, Warrington WA4 4AD, UK

² Fachbereich Physik, Martin-Luther-Universitaet Halle-Wittenberg,
Friedemann-Bach-Platz 6, D-06099 Halle, Germany

³ Institute of Physics and Astronomy, University of Aarhus,
DK-8000 Aarhus C, Denmark

⁴ Metals and Ceramics Division, Oak Ridge National Laboratory,
Oak Ridge, TN 37830, USA

⁵ INFP, Forschungszentrum Karlsruhe GmbH, Postfach 3640,
D-76021 Karlsruhe, Germany

In this talk we discuss an application of the self-interaction corrected local spin density approximation (SIC-LSD) to half-metallic transition metal oxides, and among them double perovskites and magnetite (Fe_3O_4). We show that also such simple transition metal monoxides as NiO and MnO can acquire half-metallic characteristics when doped with vacancies. We concentrate on the electronic and magnetic properties of these compounds and in magnetite, in addition, issues of charge order are also thoroughly investigated.



Centre of Excellence: Magnetic and Molecular Materials for Future Electronics

Institute of Molecular Physics, Polish Academy of Sciences
ul. Mariana Smoluchowskiego 17, 60-179 Poznań, Poland

**SELF INTERACTION CORRECTED ELECTRONIC STRUCTURE
CALCULATIONS FOR CORRELATED SYSTEMS**

W. Temmerman, Z. Szotek and M. Lueders
Daresbury Laboratory

A. Svane
Institute of Physics and Astronomy, University of Aarhus

L. Petit
Center for Computational Sciences, Oak Ridge National Laboratory

P. Strange
Department of Physics, University of Keele

A. Ernst
MPI Halle

D. Koedderitzsch
University of Halle

H. Winter
INFP, Forschungszentrum Karlsruhe

An overview is given of applications of SIC-LSD calculations for correlated d and f electron systems. In particular it is shown that SIC-LSD splits d and f bands into a manifold of localized states, occurring well below the bottom of the valence band, and a band-like manifold represented essentially by the LSD potential. This split of the states allows for the introduction of the concept of nominal valence, which is the number of electrons left on the site to participate in band formation. Examples, such as the progression of trivalent to divalent to trivalent to divalent through the rare earth series will demonstrate these concepts. In another example, using Yb compounds, a comparison will be made with a semi-phenomenological method of calculating valences. Applications to actinides and actinide compounds such as PuO₂ will be presented as well as some selected applications to d electron systems, namely YBa₂Cu₃O₇ and La_{0.7}Sr_{0.3}MnO₃. Finally we remark that SIC-LSD is a scheme well suited to describe static correlations when the electrons are well localized. A road map will be presented how to incorporate dynamic correlations.



**FRONTIERS OF NANOMAGNETISM INVESTIGATED BY SPIN-POLARIZED
SCANNING TUNNELING SPECTROSCOPY**

Roland Wiesendanger

Institute of Applied Physics and Microstructure Adv. Research Center Hamburg (MARCH)
University of Hamburg, Jungiusstr. 11, D-20355 Hamburg, Germany
<http://www.nanoscience.de>, Email: wiesendanger@physnet.uni-hamburg.de

In order to probe and tailor magnetic properties at the spatial limit we have combined the scanning tunneling microscope (STM) with spin-sensitivity [1-3]. This is achieved by the use of ferro- [4,5] and antiferromagnetically [6,7] coated probe tips offering a high degree of spin-polarization of the electronic states involved in the tunneling process. Magnetic domain imaging with sub-nanometer-scale spatial resolution has been demonstrated for magnetic transition metal [8,9] as well as rare earth metal films [10,11]. Ultra-sharp domain walls were discovered in ultra-thin iron films [12] while for ferromagnetic [13] and antiferromagnetic [14] samples, the different magnitude or orientation of magnetic moments could directly be made visible at the atomic level.

The phenomenon of magnetic hysteresis was observed for the first time at the single-digit nanometer length scale and has directly been correlated with microscopic processes of domain nucleation and domain wall motion [15]. We also studied magnetic vortex structures in mesoscopic-scale ferromagnetic systems which are of relevance for current developments in MRAM technology [7]. Magnetic switching phenomena of nano-scale magnetic islands and nanoparticles were studied by time-dependent spin-sensitive STM imaging [16]. It will be shown that granular thin films exhibit a complex magnetic switching behaviour due to the statistical distribution of grain sizes, grain shapes and inter-grain spacings.

Finally, we will discuss the application of spin-sensitive STM measurements to individual atoms and molecules on magnetic substrates [17]. In particular, we will show that both the orbital symmetry as well as the spin character of electronic scattering states around single atomic impurities can be determined from real-space spin-sensitive STM data.



Centre of Excellence: Magnetic and Molecular Materials for Future Electronics

Institute of Molecular Physics, Polish Academy of Sciences
ul. Mariana Smoluchowskiego 17, 60-179 Poznań, Poland

References:

a) Recent review articles:

- [1] R. Wiesendanger, *Current Opinion in Solid State & Materials Science* 4, 435 (1999):
Surface magnetism at the nanometer and atomic scale.
- [2] R. Wiesendanger and M. Bode, *Solid State Commun.* 119, 341 (2001):
Nano- and atomic-scale magnetism studied by spin-polarized scanning tunnelling microscopy and spectroscopy.
- [3] M. Bode and R. Wiesendanger, in: *Magnetic Microscopy of Nanostructures* (eds. H. Hopster and H.P. Oepen), Springer, Berlin, Heidelberg (2003):
Spin-Polarized Scanning Tunneling Spectroscopy.

b) Original articles:

- [4] R. Wiesendanger, H.-J. Guentherodt, G. Guentherodt, R.J. Gambino, and R. Ruf,
Phys. Rev. Lett. 65, 247 (1990):
Observation of vacuum tunnelling of spin-polarized electrons with the scanning tunnelling microscope.
- [5] M. Bode, O. Pietzsch, A. Kubetzka, S. Heinze, and R. Wiesendanger,
Phys. Rev. Lett. 86, 2142 (2001):
Experimental evidence for intra-atomic non-collinear magnetism at thin film probe tips.
- [6] A. Kubetzka, M. Bode, O. Pietzsch, and R. Wiesendanger,
Phys. Rev. Lett. 88, 057201 (2002):
Spin-polarized scanning tunnelling microscopy with antiferromagnetic probe tips.
- [7] A. Wachowiak, J. Wiebe, M. Bode, O. Pietzsch, M. Morgenstern, and R. Wiesendanger,
Science 298, 577 (2002):
Internal spin structure of magnetic vortex cores observed by spin-polarized scanning tunneling microscopy.
- [8] O. Pietzsch, A. Kubetzka, M. Bode. and R. Wiesendanger,
Phys. Rev. Lett. 84, 5212 (2000):
Real-space observation of dipolar antiferromagnetism in magnetic nanowires by spin-polarized scanning tunneling spectroscopy.



- [9] M. Kleiber, M. Bode, R. Ravlić, and R. Wiesendanger,
Phys. Rev. Lett. 85, 4606 (2000):
Topology-induced spin frustrations at the Cr(001) surface studied by spin-polarized scanning tunneling spectroscopy.
- [10] M. Bode, M. Getzlaff, and R. Wiesendanger, Phys. Rev. Lett. 81, 4256 (1998):
Spin-polarized vacuum tunneling into the exchange-split surface state of Gd(0001).
- [11] M. Bode, M. Getzlaff, A. Kubetzka, R. Pascal, O. Pietzsch, and R. Wiesendanger,
Phys. Rev. Lett. 83, 3017 (1999):
Temperature-dependent exchange splitting of a surface state on a local-moment magnet: Tb(0001).
- [12] M. Pratzner, H.J. Elmers, M. Bode, O. Pietzsch, A. Kubetzka, and R. Wiesendanger,
Phys. Rev. Lett. 87, 127201 (2001):
Atomic-scale magnetic domain walls in quasi-one-dimensional Fe nanostripes.
- [13] R. Wiesendanger, I.V. Shvets, D. Buegler, G. Tarrach, H.-J. Guentherodt, J.M.D. Coey,
and S. Graeser, Science 255, 583 (1992):
Topographic and magnetic-sensitive scanning tunnelling microscopy study of magnetite.
- [14] S. Heinze, M. Bode, O. Pietzsch, A. Kubetzka, X. Nie, S. Bluegel, and R. Wiesendanger,
Science 288, 1805 (2000):
Real-space imaging of two-dimensional antiferromagnetism on the atomic scale.
- [15] O. Pietzsch, A. Kubetzka, M. Bode, and R. Wiesendanger,
Science 292, 2053 (2001):
Magnetization reversal of Fe nanowires studied by spin-polarized scanning tunnelling spectroscopy.
- [16] M. Bode, O. Pietzsch, A. Kubetzka, and R. Wiesendanger,
submitted to Nature:
Shape dependent thermal switching behavior of superparamagnetic nanoislands.
- [17] K. von Bergmann, M. Bode, A. Kubetzka, M. Heide, S. Bluegel, and R. Wiesendanger,
submitted to Phys. Rev. Lett.:
Spin-polarized electron scattering at single oxygen adsorbates on a magnetic surface.



TEMPERATURE DEPENDENCE OF FMR LINEWIDTH AND FIELD-SHIFT IN EXCHANGE-BIASED BILAYERS

J. Dubowik^(a), I. Gościańska^(b), A. Paetzold^(c), and K. Röhl^(c)

^(a)Institute of Molecular Physics, P.A.Sci, Smoluchowskiego 17, 60-179 Poznań, Poland,

^(b)Dept. of Physics, A. Mickiewicz Univ., Umultowska 85, 61-613 Poznań, Poland,

^(c)Department of Physics, Kassel University, H. Plett Str. 40, 34132 Kassel, Germany

Thin ferromagnetic films (FM) in contact with suitably prepared antiferromagnets (AF) can exhibit a hysteresis loop shifted along the field axis. This effect of so-called exchange bias has been found to be practical in various GMR structures (e.g. spin valves). However, many of its aspects including spin dynamics still remain to be resolved.

Here results are reported of a detailed investigation of ferromagnetic resonance (FMR) in exchange-biased NiFe/NiO bilayers obtained by sputtering. A striking temperature dependence of negative and nearly isotropic field shift for both in-plane and perpendicular directions of the applied field is accompanied with pronounced maxima in temperature dependence of FMR linewidth at ~ 150 K, well below the Neel temperature of NiO. The same structures without any exchange-bias exhibit no such behavior and can serve as reference samples of the „free” FM thin films. It enables us to distinguish spin dynamics phenomena related exclusively to FM/AF interactions.

Our results are compared with previous experimental FMR [1-3] and Brillouin light scattering [4] data on various FM/AF structures and suggest that spin dynamics (spin wave damping and anomalous field shift) in the FM/AF structures can be described in a consistent way by a single mechanism of the so-called slow-relaxation [5].

This work was supported by the KBN project PBZ/KBN-044/P03-2001 and by Technological Cooperation Polish-German Project.

[1] P. Lubitz et al., J. Appl. Phys. 89 (2001) 6901

[2] M. Rubinstein et al., J. Magn. Magn. Mater. 210 (2000) 329

[3] M. Pechan et al., Phys. Rev. B 65 (2002) 064410

[4] W. S. Lew et al., J. Appl. Phys. 89 (2001) 7654

[5] see for example R. W. Teale in „Physics of magnetic garnets”, ed. A. Paoletti,

North-Holland 1978



Centre of Excellence: Magnetic and Molecular Materials for Future Electronics

Institute of Molecular Physics, Polish Academy of Sciences
ul. Mariana Smoluchowskiego 17, 60-179 Poznań, Poland

**MAGNETIC BEHAVIOUR OF CUBIC (FeNi)₂₃B₆ PHASE EMBEDDED IN
AMORPHOUS MATRIX**

B. Idzikowski^a, A. Szajek^a and J.-M. Greneche^b

^aInstitute of Molecular Physics, Polish Academy of Sciences,
M. Smoluchowskiego 17, 61-179 Poznań, Poland

^bLaboratoire de Physique de L'Etat Condensé, UMR CNRS 6087, Faculté des Sciences,
Université du Maine, 72085 Le Mans, Cedex 9, France

Due to the magnetic exchange interactions nanocrystalline systems consisting of soft magnetic phase placed in amorphous matrix can reveal a smooth magnetization curve near zero field with extremely small coercive force.

Nickel-rich amorphous precursors with chemical composition of Ni₆₄Fe₁₆Zr₇B₁₂Au₁ were produced by melt-spinning technique and then heat-treated at temperatures ranged from 420°C to 600°C for one hour to form nanostructure. The transformation from the amorphous state into the nanocrystalline state was investigated by the DSC, XRD, VSM and Mössbauer techniques. The annealing favours the emergence of cubic Fe_xNi_{23-x}B₆ crystalline grains (10-25 nm in diameter), as it was identified by XRD measurements. Magnetic measurements made at 4.2-1100 K reveal rather high value of saturation magnetisation (nearly 60 and 40 Am²/kg at 4.2 K and room temperature, respectively) in amorphous as well in nanocrystalline states. Those facts are consistent with 300K ⁵⁷Fe Mössbauer results which are well supported by the calculations of Fe and Ni magnetic moments in not substituted Ni₂₃B₆ and Fe₂₃B₆ phases, using the spin polarized tight binding linear muffin-tin orbital (*TB-LMTO*) method. The magnetic moments on Fe and Ni atoms in Fe₂₃B₆ and Ni₂₃B₆ compounds depend on their local environments. The iron magnetic moments are enhanced up to about 3 μ_B/atom and for nickel reduced, even to zero. The present study will be continued for (Fe_{1-x}Ni_x)₂₃B₆ systems to establish dependence of magnetization on concentration of Ni impurities and their site preference. After annealing ribbons became extremely magnetically soft and in a nanocrystalline state show also good mechanical properties, as compared with the FINEMET, NANOPERM or HITPERM. An improved magnetic properties and reduced brittleness of the samples offer attractive possibilities for applications of this novel Ni-rich alloy.

Acknowledgement: This work was supported by the France-Poland (CRNS-KBN) mutual agreement, Project No. 9533.



Centre of Excellence: Magnetic and Molecular Materials for Future Electronics

**Institute of Molecular Physics, Polish Academy of Sciences
ul. Mariana Smoluchowskiego 17, 60-179 Poznań, Poland**

**ELECTRONIC, MAGNETIC AND TRANSPORT PROPERTIES OF
FERROMAGNET-SEMICONDUCTOR HETEROSTRUCTURE SYSTEMS**

Michal Kosuth, Voicu Popescu, Hubert Ebert

Department Chemistry / Physical Chemistry
University of Munich, Germany

Magneto-electronics receives a lot of interest, because this research field of applied solid state physics allows one to extend the potential of electronic devices by exploiting the spin of the electrons. A very promising effect is the tunneling magnetoresistance (TMR) that denotes the observation that the tunneling current across a tunneling barrier that separates two magnetic layers depends on the relative orientation of the magnetisation of these layers. This effect could be demonstrated several years ago for a ferromagnet-insulator-ferromagnet (FM-I-FM) layer system and first prototypes of a dynamic storage chip could be presented recently. Devices based on ferromagnet-semiconductor-ferromagnet (FM-SC-FM) heterostructures seem to have several advantages compared to insulator-based tunneling junctions. The lecture will give an overview of the achievements in this area. Several examples of experimental results dealing with the magnetic properties of FM-SC systems at the interface and dealing with the spin-polarised injection will be mentioned. Most emphasis, however, will be on theoretical investigations on FM-SC heterostructure systems. The attempt of giving an explanation for the magnetic and transport properties will be followed. Correct treatment of the spin-orbit coupling leads to the possibility of calculating the magneto-crystalline anisotropy and its influence on spin-dependent transport. It will be shown that the magnetic anisotropy strongly depends on the geometry of the interface and correlates with the anisotropy of the orbital moments.



Centre of Excellence: Magnetic and Molecular Materials for Future Electronics

Institute of Molecular Physics, Polish Academy of Sciences
ul. Mariana Smoluchowskiego 17, 60-179 Poznań, Poland

**FERROMAGNETICALLY CONTACTED METALLIC CARBON
NANOTUBES WITH SPIN-SELECTIVE INTERFACES**

S. Krompiewski

Institute of Molecular Physics, Polish Academy of Sciences,
M. Smoluchowskiego 17, 60-179 Poznań, Poland

Spin-dependent transport through single-wall armchair carbon nanotubes (SWCNT) is studied theoretically within the single-band tight-binding model, by means of the Green's function partitioning technique. The emphasis is put on the effect of an extra magnetic monolayer at the electrodes on electrical conductance and giant magnetoresistance (GMR). In order to meet the charge neutrality requirement – the so-called extended molecule concept has been used. It has been shown that in the case when the monolayers have got enhanced magnetic moments and are antiferromagnetically exchange-coupled to the electrodes, the GMR value can approach 100%, i.e. both the spin-dependent conductance channels may become blocked in the anti-aligned electrodes configuration. A remarkable feature of the conductance spectra is that they reveal to a large degree the “finger prints” of the SWCNTs. In particular, the conductance spectra peaks are separated from one another roughly as in isolated nanotubes. It has been also shown that the GMR-effect is very sensitive to the relative band line-up of electrodes and nanotubes, what on the one hand explains a poor reproducibility of experimental results, and on the other hand makes it possible to control the GMR with a gate voltage.



Centre of Excellence: Magnetic and Molecular Materials for Future Electronics

Institute of Molecular Physics, Polish Academy of Sciences
ul. Mariana Smoluchowskiego 17, 60-179 Poznań, Poland

FAST MAGNON RELAXATION

J.A. Morkowski

Institute of Molecular Physics, Polish Academy of Sciences, Poznan, Poland

Magnon relaxation times are usually calculated by solving linearized Boltzmann-type equation for magnon occupation numbers. If in the initial state the occupation number of a particular magnon mode is high, non-linear terms in the Boltzmann equation strongly enhance the short-time relaxation rate for that magnon mode. The problem will be discussed in details for a case of three-magnon confluence processes for degenerate magnon spectrum. The same qualitative features characterize higher order relaxation processes like the four-magnon ones.



Centre of Excellence: Magnetic and Molecular Materials for Future Electronics

Institute of Molecular Physics, Polish Academy of Sciences
ul. Mariana Smoluchowskiego 17, 60-179 Poznań, Poland

AB INITIO SIMULATIONS OF MOLECULAR MAGNETS

Andrei Postnikov

Universitaet Osnabrueck - Fachbereich Physik

D-49069 Osnabrueck, Germany

A remarkable increase in the number of studies on molecular magnetic systems during the last decade is clearly related to the progress in chemistry of such systems. Different families of molecular magnets have been synthesized, their crystal structure determined, their magnetic properties analyzed.

For the theory, such systems provide an interesting playground accessible from the side of model systems (“exact” diagonalisation within, e.g., Heisenberg model), as well as from the side of quantitative calculation from first principles. The shortcomings of these two approaches are the neglect of true chemical environment and bonding (in the models) and probably insufficient, or not accurate enough, incorporation of correlation effects (in the density functional theory-related schemes). The chemical complexity of molecular magnets precluded so far their “straightforward” simulation in a calculation approaches of superior accuracy, like quantum Monte Carlo. Therefore it is not *a priori* clear to which extent one or other of “ideologies” now in use will be more valid, or useful - whether an overlap will take place in describing the relevant physics from different point of view, or a gap in between would still leave some essential features unexplored. After a brief introduction to the experimental evidence and the progress with the Heisenberg model for such systems, I'll discuss in detail the situation with density functional calculations. Here one must note that the advent of molecular magnets did not necessarily demand for the development of essentially new calculation schemes, so that a decades-long progress in quantum-mechanical study of small clusters and molecules could be made use of, and extrapolated further, with the natural rise in computer power. However, molecular magnets turn out to be hard cases for computational treatment for different reasons in different established calculation approaches.

The openness of crystal structure demands for one or another “full-potential” formalism, leaving traditional muffin-tin- or atomic sphere approximation-based tools out of the market. The presence of transition metals and/or other constituents with important deep semicore states creates problems for pseudopotential planewave methods. Moreover, the need for a large (albeit largely empty) “simulation box” around a molecule makes planewave-related methods expensive. An abundance of hydrogen and hence strong disbalance in atom “sizes” makes it hard for linearized augmented plane wave scheme. The often unusual chemical composition reduces the usefulness of *a priori* tuned basis sets in those tight-binding-type methods which heavily depend on pre-adjusted basis functions for their efficiency. Simultaneously, the options to treat non-collinear spin-density distribution and to have accurate forces on atoms for studying structure relaxation and dynamics may be advantageous and sometimes necessary. As a consequence, flexible, efficient and accurate methods (and codes) are in the demand, of which several have been successfully applied to systems of reasonable complexity. After an overview of situation in this field, a detailed analysis will be given of our recent results.

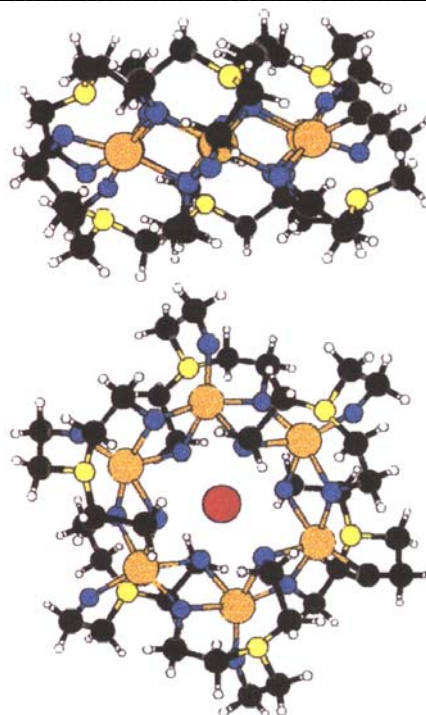


Centre of Excellence: Magnetic and Molecular Materials for Future Electronics

Institute of Molecular Physics, Polish Academy of Sciences

ul. Mariana Smoluchowskiego 17, 60-179 Poznań, Poland

As an example of a system of practical interest we consider hexanuclear “ferric wheel” $\text{LiFe}_6[\text{N}(\text{CH}_2\text{CH}_2\text{O})_3]_6\text{Cl}$ (see figure) synthesized at the Institut fuer Organische Chemie in Erlangen [1], along with other systems with differently bonded Fe atoms. The calculation have been done by the *Siesta* method [2], which employs density functional theory and numerical basis orbitals. A large number of electronic states within narrow energy interval and the effective lack of useful crystal symmetry results in a strong nearly-degeneracy of electronic states in the vicinity of the band gap (or, of the Fermi level). This makes the convergence of electronic structure calculation extremely difficult. The imposition of a fixed spin moment constraint help however to improve convergence by suppressing electron density fluctuations between two spin channels.



According to both local density (LDA) and generalized gradient (GGA) approximations, local magnetic moments of $4 \mu_B$ persist on Fe sites irrespectively of actual magnetic arrangement - ferromagnetic, inverted spin on one or several atoms, or interchanging antiferromagnetic ordering in the ring, the latter (correctly) turning out to be the ground state. It became commonplace to refer to “ferric wheels” and other related systems as those with $S=5/2$ per Fe atom, on the basis of magnetization measurements, whence the chemical state Fe^{3+} is derived. The calculations indicate that the situation is more complicated than that. In particular, Fe $3d$ states are *not* fully localized but participate in a covalent bonding with neighbouring oxygen atoms (that holds the molecule together). Whereas majority-spin $3d$ states of Fe are fully occupied, minority-spin subband is not empty but contains about one electron on the Fe-O bonds. The description of electronic structure as obtained in the calculation (also, the absence of clearly Fe^{3+} behaviour) is consistent with available experimental data from photoemission and soft X-ray emission.

The magnetic polarization of the triethanolamin group hosting each Fe atom, however, amounts to $1 \mu_B$, and the resulting spin of, indeed, $S=5/2$, albeit delocalized, behaves nevertheless as a rigid one, experiencing a reversal when a magnetic configuration changes. This behaviour maps well onto the Heisenberg model and allows to estimate exchange parameters from total energies of different magnetic configurations. The estimates of about -80 K are of correct sign and order, but somehow larger magnitude than those derived from neutron scattering data [3]. An inclusion of local correlation effects within the LDA+*U* scheme or similar doesn't seem probable to change the situation qualitatively, but would tend to reduce the interaction parameters, as the band gap gets larger.

References

- [1] R. W. Saalfrank *et al.*, *Angew. Chem.* **109** (1997) 2596.
- [2] J. M. Soler *et al.*, *J. Phys. Cond. Matter* **14** (2002) 2745.
- [3] O. Waldmann *et al.*, *Inorg. Chem.* **38** (1999) 5879.



FE-BASED SPIN ALIGNERS GROWN ON SEMICONDUCTING SUBSTRATES

Marek Przybylski

*Max-Planck-Institut fuer Mikrostrukturphysik, Weinberg 2, 06120 Halle, Germany
and*

*Solid State Physics Department, Faculty of Physics and Nuclear Technics,
AGH University of Science and Technology, Mickiewicza 30, 30-059 Krakow, Poland*

The possibility of realizing devices by exploiting the electron's property of possessing a spin has captured physicist attention since the past decade. A variety of Fe-based multilayer structures for a magnetic recording or exchange-biased media have been grown, mostly on MgO substrates. From the point of view of magneto-electronics applications it is preferable to combine the structure with a semiconducting substrate. Recently, an attempt has been made to avoid the formation of "magnetically dead layers" in Fe films epitaxially grown on a number of semiconductors. A variety of phenomena observed for Fe-based spin aligners grown on an atomically flat (4x6)-like reconstructed GaAs(001) surface is reviewed.

Antiferromagnetically (AFM)-coupled Fe/Cr/Fe trilayers, epitaxially grown on GaAs(001), reflect magnetic anisotropy of the GaAs(001)/Fe system characterized by uniaxial anisotropy of the easy-axis of magnetization along the [110] direction. This allows growth of an artificial "layered antiferromagnet" exhibiting uniaxial magnetic anisotropy with minimal material and technological complexities. When such a $(\text{Fe/Cr/Fe})_{\text{AFM}}$ structure is completed by another Fe layer separated with another Cr-spacer, the low field magnetization signal from the $(\text{Fe/Cr/Fe})_{\text{AFM}}/\text{Cr/Fe}$ sample corresponds to the top Fe layer only. A strong increase of coercivity is found at low temperatures and 90° interface coupling is detected. In the case of $(\text{Fe/Cr/Fe})_{\text{AFM}}$ trilayers of different thickness of the Fe layers, "reversed" minor ellipticity loops are measured with longitudinal MOKE. This behavior is interpreted by depth variation of the MOKE sensitivity.

Theoretical work predicts that efficiency of the spin injection from a ferromagnet into a semiconductor can be improved for electrons created by tunneling, since such a process is not affected by the conductivity mismatch and results in conservation of the spin polarization. For single-crystalline Fe/MgO/Fe junctions grown on GaAs(001), magnetization of one of the Fe electrodes is pinned by its AFM-coupling to another Fe layer $((\text{Fe/Cr/Fe})_{\text{AFM}})$ over a field range controlled by the thickness relation between both Fe layers in the $(\text{Fe/Cr/Fe})_{\text{AFM}}$ structure. Another approach for the independent magnetization switching is realized by differing coercivity of the Fe layers. The coercivity of the top Fe electrode can be increased due to crystallographic defects created e.g. by covering with Ni. We have shown that the interlayer coupling between the Fe electrodes is weak for MgO thicknesses down to about 4ML. It is difficult to reach a structure quality sufficient to detect a pure AFM-exchange interaction expected for the interlayer coupling across a non-metallic spacer. Regardless of the preparation conditions, below 2.5ML of MgO the coupling is dominated by pinholes and "orange peel" effect.

Magnetic systems exhibiting perpendicular anisotropy are of particular interest for a potential perpendicular emission of circularly polarized photons resulting from spin injection and electron-hole recombination in a semiconductor. For this purpose, ultrathin Ni films were grown on GaAs(001). Deposition of about 1ML of Fe on the top of GaAs(001)/Ni recovers the LEED pattern which is not visible after deposition of several ML of Ni. The Ni/Fe system exhibits out-of-plane magnetization at low temperature. Another approach for perpendicular magnetization is realized via growth of the $L1_0$ ordered alloys by alternating deposition of Fe and Au (or Pt) atomic layers on top of the Au (or Pt) buffer layer.



Centre of Excellence: Magnetic and Molecular Materials for Future Electronics

Institute of Molecular Physics, Polish Academy of Sciences

ul. Mariana Smoluchowskiego 17, 60-179 Poznań, Poland

**MAGNETOCRYSTALLINE ANISOTROPY OF
STRAINED TRANSITION METALS AND RARE-EARTH INTERMETALLICS:
DENSITY FUNCTIONAL CALCULATIONS**

Manuel Richter

Dept. of Theoretical Solid State Physics, IFW Dresden,
P.O. Box 270016, D-01171 Dresden, Germany

The magnetocrystalline anisotropy (MA) energies of strained hcp Fe and Co, bct Fe, RCo_5 ($R = \text{Y, La, Pr, Nd, Sm, Gd}$) and R_2T_{17} ($R = \text{Y, Sm; T = Fe, Co}$) have been determined by means of relativistic density functional calculations, including orbital polarization corrections. The obtained MA energies agree well with available experimental data. They are found to be strongly affected by changes of the lattice geometry (c/a ratio and volume) and substitutions, as a consequence of band structure and band filling effects.



Centre of Excellence: Magnetic and Molecular Materials for Future Electronics

**Institute of Molecular Physics, Polish Academy of Sciences
ul. Mariana Smoluchowskiego 17, 60-179 Poznań, Poland**

MAGNETORESISTANCE OF Ni-Fe/Au/Co/Au MULTILAYERS

F. Stobiecki^(a), B. Szymański^(a), T. Luciński^(a), J. Dubowik^(a), M. Urbaniak^(a), and K. Roell^(b)

^(a)Institute of Molecular Physics, PAS, Smoluchowskiego 17, 60-179 Poznań, Poland

^(b)Department of Physics, Kassel University, H. Plett Str. 49, 34132 Kassel, Germany

For particular applications different magnetoresistive elements, i.e., sensors with required $R(H)$ dependence are necessary. Therefore, a large number of artificial thin film structures have been investigated. In result structures such as spin-valves (applied as read heads) or pseudo-spin-valves (optimal for RAM memory cells) were elaborated. For all these structures the giant magnetoresistance (GMR) effect is accompanied by switching from antiparallel to parallel magnetization configuration in ferromagnetic layers.

In this contribution the investigations concerning the new type of layered structures, characterized by alternating out-of-plane and in-plane magnetization configurations in ferromagnetic layers in the remanence state, will be demonstrated. To realize such structures the set of $(\text{Py}/\text{Au}/\text{Co}/\text{Au})_{15}$ (Py = Permalloy = $\text{Ni}_{83}\text{Fe}_{17}$) multilayers were deposited on glass substrates using the UHV magnetron sputtering. Permalloy and Co were chosen since Py posses a pronounced in-plane anisotropy whereas thin Co layers sandwiched between Au have a strong perpendicular anisotropy [1-3]. The exemplary VSM hysteresis loops and $\text{GMR}(H)$ ($\text{GMR}(H) = 100\%[R(H)-R(2T)]/R(2T)$; $R(H)$ and $R(2T)$ are the resistance at magnetic field H and $H = 2T$) dependences are shown in Fig.1. For a thickness of gold layers $t_{\text{Au}} > 1.5$ nm the magnetization reversals of the Co and Py layers are independent (the layers are almost completely decoupled) and can be easily recognized in hysteresis loops measured for magnetic field applied in-plane (H_{\parallel}) and perpendicular to the plane (H_{\perp}) (Fig. 1 a, b). The central portions of hysteresis loops for H_{\parallel} and H_{\perp} correspond to Py and Co reversal, respectively. Neglecting the range of small fields, the magnetization of Py (Co) layer always points in the field direction for H_{\parallel} (H_{\perp}) and only magnetization of Co (Py) layer rotates from the perpendicular (in-plane) to the field direction. Thus, the changes of $\cos\varphi(H)$ (φ is the angle between magnetization directions of Py and Co layers) and in consequence the changes of $\text{GMR}(H)$ are only related to magnetization reversal of one layer, namely Py for H_{\perp} or Co for H_{\parallel} . Due to the uniaxial perpendicular anisotropy of Co layers and in-plane shape anisotropy of Py layers linear $\text{GMR}(H)$ dependences are observed both for H_{\parallel} and H_{\perp} (Fig. 1 c, d). This behavior of investigated structures can be applied for quantitative measurements of magnetic field.

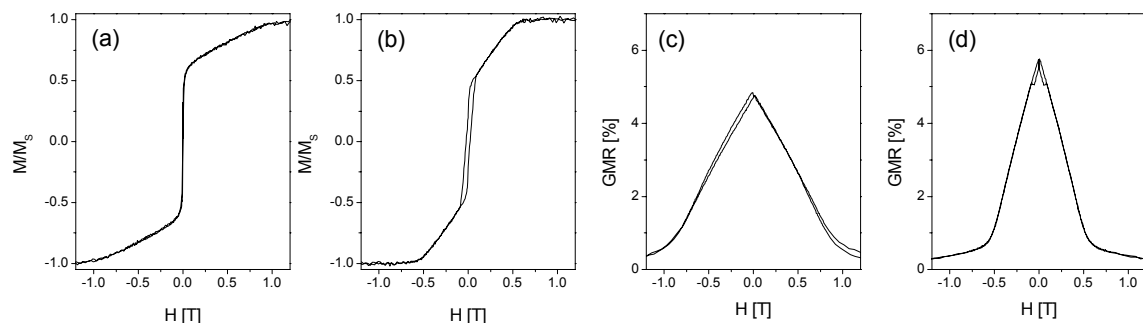


Fig. 1. Hysteresis loops (a, b) and magnetoresistance curves (c, d) of $(\text{Ni}_{83}\text{Fe}_{17}\text{-}2\text{nm}/\text{Au}\text{-}3\text{nm}/\text{Co}\text{-}0.6\text{nm}/\text{Au}\text{-}3\text{nm})_{15}$ multilayers measured for magnetic field applied in plane H_{\parallel} (a, c) and perpendicular to sample plane H_{\perp} (b, d), respectively.



To optimize the structure and to determine the influence of the thickness (t) of particular layers on $GMR(H)$ dependences the following series of samples were studied:

- i) (Py-2nm/Au-3nm/Co- t_{Co} /Au-3nm)₁₅ ($0.2 \leq t_{Co} \leq 1.5$ nm),
- ii) (Py-2nm/Au- t_{Au} /Co-0.6nm/Au- t_{Au})₁₅ ($0.5 \leq t_{Au} \leq 3$ nm),
- iii) (Py- t_{Py} /Au-2nm/Co-0.6nm/Au-2nm)₁₅ ($1 \leq t_{Py} \leq 4$ nm).

The results concerning GMR values as a function of cobalt, gold and Permalloy thickness are demonstrated in Fig. 2 and can be summarized as follows:

- $GMR(t_{Co})$ (Fig. 2a) – the optimal thickness of Co layers lies in the range $0.4 \leq t_{Co} \leq 1.2$ nm, i.e., in the range assuring perpendicular anisotropy and continuous structure of Co layers.
- $GMR(t_{Au})$ (Fig. 2b) – for $t_{Au} \leq 1.25$ nm the GMR effect strongly decrease due to increasing ferromagnetic coupling between Co and Py layers (in consequence $\varphi < \pi/2$ at $H=0$), the slow decrease of GMR for $t_{Au} \geq 1.5$ nm is related to the increasing scattering of conduction electrons and to increasing shunting of the current in Au layers [4].
- $GMR(t_{Py})$ (Fig. 2c) – the dependence shows a weak maximum for $t_{Py} \approx 3$ nm typical of all GMR structures containing Py [4, 5].

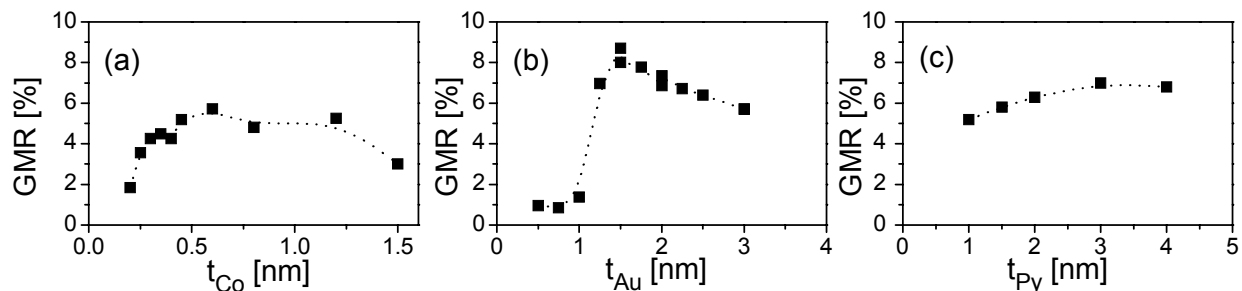


Fig. 2. GMR value of (Py/1Au/Co/Au)₁₅ multilayers as a function of cobalt (a), gold (b) and Permalloy (c) layers thickness.

Finally, it should be noted that for the investigated structures the saturation fields of $GMR(H_{\perp})$ and $GMR(H_{\parallel})$ dependences can be tuned by varying thickness of Py and Co layers, respectively. For appropriate layers thickness the magnetoresistance response of the structure can be nearly isotropic (Fig. 3).

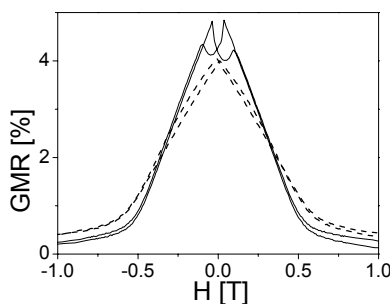


Fig. 3. $GMR(H)$ dependence of (Py-2nm/Au-3nm/Co-0.8nm/Au-3nm)₁₅ for magnetic field applied in-plane (dash line) and perpendicular to the plane.

- [1] C. Chappert et al., Phys. Rev. B **34** (1986) 3192.
- [2] J. Dubówik et al., phys. stat. sol. (a) **196** (2003) 41.
- [3] F. Stobiecki et al., J. Magn. Magn. Mater. **239** (2002) 276.
- [4] B. Dieny, J. Magn. Magn. Mater. **136** (1994) 335.
- [5] T. Luciński et al. J. Magn. Magn. Mater. **174** (1997) 192.



LARGE INTERFACE SCATTERING FROM FIRST PRINCIPLES

M. Zwierzycki^{1,4}, M. Talanana¹, K. Xia⁵, P.J. Kelly¹, G.E.W. Bauer²

¹ University of Twente, Enschede, The Netherlands

² Delft University of Technology, The Netherlands

⁴ Institute of Molecular Physics, Poznań, Poland

⁵ State Key Laboratory for Surface Physics, Beijing, China

The open 3d shells of the transition metal atoms used to make magnetic multilayers give rise to complex band structures which have to be taken into account in any quantitative estimation of the interface scattering whose spin-dependence determines the remarkable transport properties of these structures. Using the TB-LMTO surface Green's function method we study a number of metallic and hybrid (metal/semiconductor) interfaces and interpret their transmittivity in terms of the electronic structures of the component materials. The efficiency of the TB-LMTO method allows us to treat disordered layers using large lateral supercells and allows us to unravel the contribution of various factors to the final transmission.



Centre of Excellence: Magnetic and Molecular Materials for Future Electronics

Institute of Molecular Physics, Polish Academy of Sciences
ul. Mariana Smoluchowskiego 17, 60-179 Poznań, Poland

MOESSBAUER EFFECT STUDY OF ATOMIC DISORDER IN Fe₂TiSn ALLOY

J.E. Frąckowiak, J. Deniszczyk

Institute of Physics and Chemistry of Metals, Silesian University
40-007 Katowice, Bankowa 12, Poland

The recent discovery of Fe₂TiSn alloy has simulated a renewal of interest in studying the effect of the local environment on the electronic and magnetic properties of the Heusler-type compounds. It was shown that Fe₂TiSn alloy belongs to the group of system in which the weakly ferromagnetic and probably heavy fermion behavior is induced by atomic disorder [1-3]. The abnormal change of the slope in the experimental lattice parameter a is observed at 240 K [1]. This anomalies provide evidence of an isostructural phase transition which could be created by an atomic disorder. The band structure calculation [4] predicts that the substitution of Fe atoms onto titanium or tin position in L2₁ structure leads to an occurrence of magnetic moment in Fe₂TiSn alloy.

The aim of present study was to investigate an effect of local atomic disorder in Fe₂TiSn alloy on the hyperfine parameters of ⁵⁷Fe and ¹¹⁹Sn nuclei by Moessbauer spectroscopy. An Fe₂TiSn ingot was prepared by arc melting the constituent metals on the water-cooled copper hearth in a high-purity argon atmosphere. The sample was annealed at 1073 K for 10 hours and then quenched in water. The iron and tin Moessbauer spectra was recorded from 80 to 300 K in a Nitrogen Liquide cryostat. The stability of the sample temperature was about 0.5 K. The Moessbauer spectra were fitted with a least-squares method program using the Gauss-Legendre technique for evaluation of the transmission integral.

The direct evidence for crystallographic disorder on an atomic scale comes from Moessbauer measurements. A single broad and asymmetric absorption lines are observed both for Fe and Sn nucleus in the investigated range of temperature. An analysis shows that to fit the ⁵⁷Fe spectra at least the one magnetic component (sextuplet) and the one paramagnetic component (single line) is required. Figure 1 presents the temperature dependence of the ⁵⁷Fe isomer shift, IS, for magnetic (M) and paramagnetic (P) components.

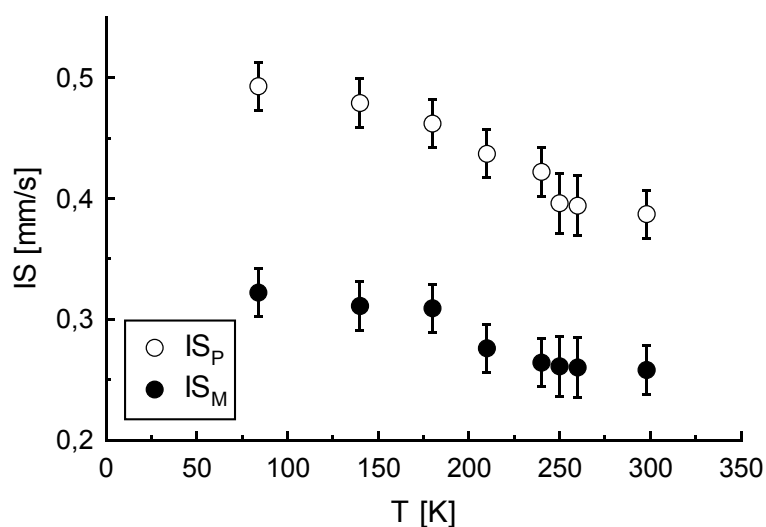


Fig. 1. The temperature dependence of the ⁵⁷Fe isomer shift for Fe₂TiSn alloy.



The observed at 240 K drop in IS_p curve provide evidence of a phase transition in the paramagnetic phase. The ^{119}Sn Moessbauer spectra of Fe_2TiSn measured at room temperature in a longitudinal field of 0.25 T show a Zeeman splitting with the value of magnetic field about 32 kGs. The experimental hyperfine parameters are compared with theoretical ones resulted from the band structure calculation using TB-LMTO method.

References

1. A. Ślebarski, M.B. Maple, E.J. Freeman, C. Sirvent, D. Tworuszka, M. Orzechowska, A. Wrona, A. Jezierski, S. Chiuzaian, M. Neumann, *Phys. Rev. B* **62** (2000) 3296.
2. A. Ślebarski, A. Wrona, T. Zawada, A. Jezierski, A. Zygmunt, K. Szot, S. Chiuzaian, M. Neumann, *Phys. Rev. B* **65** (2002) 144430.
3. S.V. Dordevic, D.N. Basov, A. Ślebarski, M.B. Maple, L. Degiorgi, *Phys. Rev. B* **66** (2002) 75122.
4. A. Jezierski, A. Ślebarski, *J. Magn. Magn. Mater.* **223** (2001) 33.



**EFFECT OF THE LOCAL ENVIRONMENT ON THE ELECTRONIC AND
MAGNETIC PROPERTIES OF $\text{Fe}_{3-x}\text{Cr}_x\text{Al}$ AND $\text{Fe}_{3-x}\text{Cr}_x\text{Si}$**

A. Go^a, M. Pugaczowa-Michalska,^b L. Dobrzyński^{a,c}

^a*Institute of Experimental Physics, University of Białystok, Lipowa 41, 15-424 Białystok, Poland*

^b*Institute of Molecular Physics, Polish Academy of Science,*

Smoluchowskiego 17, 60-179 Poznań, Poland

^c*The Soltan Institute for Nuclear Studies, 05-400 Otwock-Świerk, Poland*

Fe_3Si and Fe_3Al alloys doped with transition metal atoms were investigated many times by different experimental and theoretical techniques. Both Fe_3Si and Fe_3Al crystallise in DO_3 -type structure (Fig.1). This structure can be interpreted as four interpenetrating *f.c.c.* Bravais lattices translated by $(1/4, 1/4, 1/4)$ vector and abbreviated A, B, C and D. In the perfectly ordered compound aluminium or silicon atoms occupy D positions. There are two non-equivalent types of iron in (A,C) position and in B position. One of them – (A,C) position has eight Fe nearest neighbour in an octahedral configuration, the second one – B site – is surrounded by four Fe and four Si or Al atoms. Transition metal atoms preferentially occupy one type of these sites, depending of their positions in the periodic table of elements. Atoms of elements that are placed on the left-hand side of iron preferentially locate at B-sites, however, atoms which are on the right side of iron demonstrate strong preference for (A,C) positions in DO_3 -type structure.

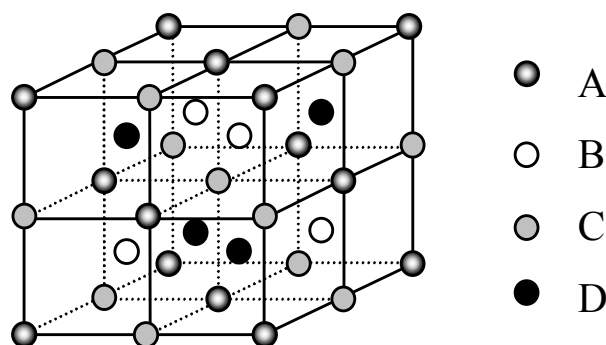


Fig.1. The DO_3 -type structure.



The aim of paper is to investigate an influence of the local surrounding of iron on its magnetic moment, hyperfine field and density of states in compounds where iron is substituted by chromium. The chromium concentration in both of alloys changes in range from $x=0$ to $x=0.5$. In order to test the influence of the local environment on electronic and magnetic properties in $\text{Fe}_{3-x}\text{Cr}_x\text{Al}$ and $\text{Fe}_{3-x}\text{Cr}_x\text{Si}$ magnetic contribution of all possible configurations in the nearest neighbour's shell for Fe(A,C) and Fe(B) sites are analysed. The presence of chromium atom in the nearest neighbourhood causes strong decrease of the magnetic moment and hyperfine field on iron. The total magnetic moments as well as the magnetic moments of chromium and iron decrease almost linearly with the concentration of chromium in considered alloys. The relationship between magnetic moments and hyperfine fields intensities is studied in detail.

The electronic structure and magnetic properties are calculated method within the framework of the local spin density approximation (LDA) by the spin-polarised self-consistent tight-binding linearized muffin-tin orbital method (TB-LMTO) in the atomic sphere approximation (ASA) for the experimental values. In present calculation the supercell structure with 32 atoms in the cell was used. The supercell structure can be divided into 32 simple cubic sublattices. Eight of them are occupied by Si or Al atoms (D positions), whereas Fe and Cr randomly occupy the remaining sublattices (A, B, C positions).



**SINGLE-ION ANISOTROPY EFFECTS IN THE
SUPRAMOLECULAR ASSEMBLY Ni₁₂**

Monika Haglauer¹, Grzegorz Kamieniarz¹, Alvaro Caramico D'Auria² and Filippo Esposito²

¹ Computational Physics Division, Institute of Physics, A. Mickiewicz University,
ul. Umultowska 85, 61-614 Poznań, Poland

² Dipartimento di Scienze Fisiche, Università di Napoli "Federico II", Piazzale Tecchio,
80125 Napoli and INFN Unità di Napoli, Italy

E-mail: gjk@amu.edu.pl (G. Kamieniarz) and filesp@na.infn.it (F. Esposito)

The Ni₁₂(O₂CMe)₁₂(chp)₁₂(H₂O)₆(THF)₆ cluster [1] (Ni₁₂ in short) is a dodecanuclear metallocyclic complex containing a ring of twelve S=1 Ni ions bridged by intersecting Ni₂O₂ rings. Such clusters are not subject to significant intermolecular interactions. Measurements of the effective magnetic moment for T > 4.2 K and a subsequent approximate analysis, have shown that the magnetic properties of Ni₁₂ can be explained by a ferromagnetic coupling inside the ring, estimated as J=13.5 K [1].

Characterization of polynuclear magnetic aggregates remains a challenging task. They have well defined molecular weights and crystal structures [2], allowing quantitative comparison of experimental results with theory. Unlike other assemblies of small magnetic particles with size and/or shape distributions, a typical sample of a molecular magnetic compound is composed of nominally identical non-interacting magnets with a unique set of chemically determined parameters. They are complex organometallic systems, too difficult to approach by the *ab initio* methods applicable to simple metal clusters.

To characterize the Ni₁₂ cluster, we consider the spin S=1 rings in the framework of the Heisenberg model with the earlier neglected single-ion anisotropy [3] and we apply the diagonalization method exploiting the point-group symmetry. Our diagonalization method, implements the idea of applying the corresponding shift operator to take into account the translational (or rotational) symmetry. This idea and the group-theory arguments enable an effective coding to be achieved and provide a reduction of the corresponding invariant subspaces, even in the presence of anisotropy for the rings size N=12, so that the numerical diagonalization of the Hamiltonian describing Ni₁₂ can be accomplished.

We calculate the corresponding energy spectra, and discuss, using the perturbative calculations, the level crossing in the presence of the applied field. A comparison with the experimental data is also performed [3].

References

- [1] Blake A.J., Grant C.M., Parsons S., Rawson J.M. and Winpenny R.E.P. 1994
J. Chem. Soc., Chem. Commun. 2363
- [2] Gatteschi D., Caneschi A., Pardi L. and Sessoli R. 1994 *Science* **265** 1054
- [3] Kamieniarz G., Matysiak R., Caramico D'Auria, Esposito F. and Benelli C. 2001
Eur. Phys. J. **23**, 183-189



**LARGE CeCu₂Si₂ SINGLE CRYSTALS FOR MAGNETIC NEUTRON
SCATTERING**

H. S. Jeevan¹, M. Deppe¹, O. Stockert¹, E. Faulhaber² and C. Geibel¹

¹ Max-Planck-Inst. for Chem. Physics of Solids, Nothnitzer Str, 40, 01187 Dresden, Germany

² TU Dresden, IAPD, D-01062 Dresden, Germany.

The discovery of superconductivity in CeCu₂Si₂ in 1979 opened the field of unconventional superconductivity in strongly correlated systems. Later on, another unconventional phase, the A-phase, of presumably magnetic character was found to compete with the superconducting phase in CeCu₂Si₂. Despite more than 20 years of intensive research, the nature of the superconducting phase and of the A-phase as well as the interaction between both are very far from being understood. A major problem is the lack of large single crystals with well defined physical properties. This prevents e.g. a study of the magnetic structure and magnetic excitations of this compound with neutron scattering, which would allow a much deeper insight into the nature of these unconventional phases. Thus despite several attempts, no magnetic Bragg peaks could yet be observed for the unconventional A-phase. The main problem in obtaining large single crystals of CeCu₂Si₂ with well defined physical properties is the peritectic formation of this compound, and the extreme sensitivity of its physical properties to tiny changes in the composition. We have grown large single crystals of CeCu₂Si₂ using a self flux method in oxide crucibles. The structure of the single crystals, their composition and their physical properties were investigated by XR-diffraction, microprobe and resistivity as well as specific heat measurements, respectively. We observed correlations between growth parameters, composition of the single crystals, and their physical properties. By tuning the growth parameters, we could grow large (~1cm³) single crystals of CeCu₂Si₂ showing either a stable A-phase ground state, a stable superconducting ground state or a competition between both phases. With these single crystals, we were now able to detect the magnetic Bragg peaks of the A-phase in pure CeCu₂Si₂. This shall allow a detailed study of this unconventional magnetic phase and of its interaction with the superconducting state.



Centre of Excellence: Magnetic and Molecular Materials for Future Electronics

Institute of Molecular Physics, Polish Academy of Sciences
ul. Mariana Smoluchowskiego 17, 60-179 Poznań, Poland

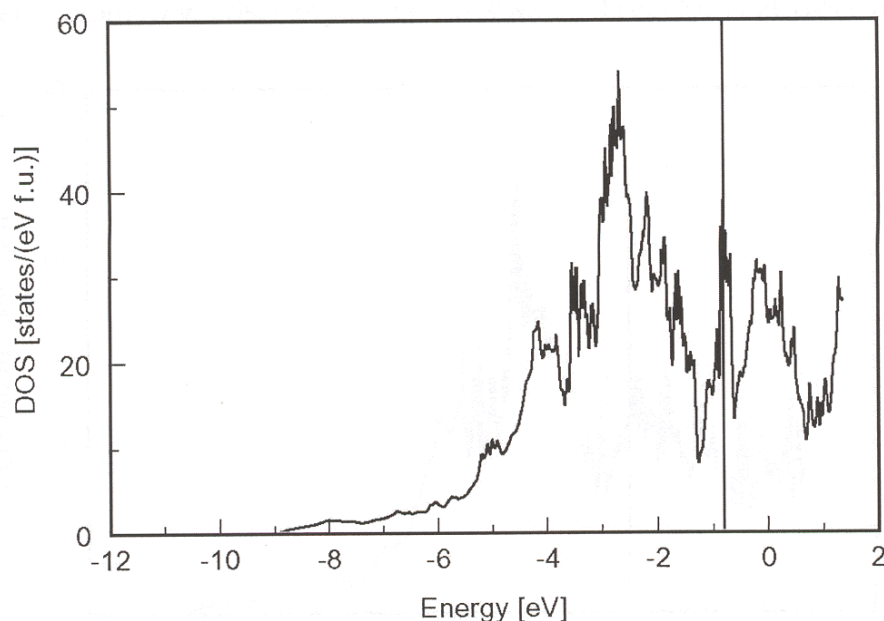
MAGNETISM AND BAND STRUCTURE OF Co/Ti MULTILAYERS

Andrzej Jezierski and Piotr Napierała

Institute of Molecular Physics, Polish Academy of Sciences, Poznań, Poland

An effect of local atomic disorder on the electronic structure and magnetic moments in $\text{Co}_{1-x}\text{Ti}_x$ systems is studied by ab-initio methods. Co-Ti alloys belong to the group of the systems in which the magnetic properties dependent strongly on the distribution of atoms in the cell. The band structure is calculated by the spin-polarised TB LMTO and SPR-KKR-CPA methods. The Co and Ti atoms are distributed in the different crystallographic structures (fcc, hcp, bcc and $L2_1$). We studied the change of the electronic structure of CoTi during the transformation from fcc to bcc structure(Bain path). We found the dependence of the total energy on the ratio of c/a . For BCC structure($c/a=1$) energy was the highest and the lowest energy was obtained for FCC structure ($c/a=1,41$). For each crystallographic structure the electronic and magnetic properties were calculated for the different distributions of Co and Ti atoms in unit cell. The calculations indicate that that magnetic moment of Co decreases about 50% near Ti layer. The density of states on the Fermi level in Co-Ti systems strongly depends on the concentration of Co atoms, as well on the distribution of Co and Ti atoms in the unit cell for the given concentration.

The figure is plotted the total density of states for $\text{Co}_{0.62}\text{Ti}_{0.38}$ in $L2_1$ type structure.



***AB-INITIO* CALCULATIONS OF THE PROPERTIES OF THE HEUSLER ALLOY**

NiMnSb

Marjana Ležaić, Gustav Bihlmayer, and Stefan Bluegel

IFF, Forschungszentrum Juelich, D-52425 Juelich, Germany

Spin-gap materials, presenting 100% spin polarisation at the Fermi level, are presently receiving much of attention because of their potential use in spintronics devices. A class of such materials are the Heusler alloys. Here we present a theoretical study of the Heusler alloy NiMnSb. In particular, we show the complex band structure as a tool for understanding of surface and interface states, and we calculate the properties of the interface with InP. We investigate the influence of the spin-orbit interaction in bulk and at the surfaces. Finally, we calculate the Curie temperature using frozen magnon excitations.



Centre of Excellence: Magnetic and Molecular Materials for Future Electronics

Institute of Molecular Physics, Polish Academy of Sciences
ul. Mariana Smoluchowskiego 17, 60-179 Poznań, Poland

ANTIFERROMAGNETIC EXCHANGE COUPLING IN $\text{Fe}/\text{Si}_x\text{Fe}_{1-x}$ MULTILAYERS

T. Luciński^(a), P. Wandziuk^(a, b), M. Urbaniak^(a), B. Andrzejewski^(a)

^(a)Institute of Molecular Physics, PAS, M. Smoluchowskiego 17, 60-179 Poznań, Poland

^(b)Poznań University of Technology, Nieszawska 13A, 60-965 Poznań, Poland

Metal-semiconductor multilayers (MLs) are extensively studied because of their potential application in electronics. Recently the investigations have been focused on Fe/Si/Fe coupled heterostructures since they show a very strong antiferromagnetic (AF) interlayer coupling [1]. In spite of many efforts, the origin of the interlayer coupling in Fe/Si system has not been clarified [2-5]. Moreover, it is not well understood how the iron-silicides formation affects the interlayer coupling. Therefore the information about the spacer layer composition and its correlation with magnetic properties of this system is of particular interest.

The $[\text{Fe}(3 \text{ nm})/\text{Si}_x\text{Fe}_{1-x}(d_S)] \times 15$ multilayers, (where $\text{Si}_x\text{Fe}_{1-x}$ alloys for $x=1, 0.66, 0.5$ and 0.4 simulate Si and FeSi_2 , FeSi , Fe_5Si_3 iron-silicide phases, respectively and d_S denotes the spacer layer thickness) were deposited in UHV by d.c. magnetron sputtering at room temperature onto oxidized Si wafers. The crystalline structure of our samples and their multilayer periodicity were examined using the high- and small-angle X-ray diffraction, respectively. Magnetization measurements were performed in the as-deposited state and after sequential annealing at 100°C and 220°C as a function of temperature ranging from 4.2 K to 300 K.

We have found that the spacer layer with $\text{Si}_{40}\text{Fe}_{60}$ composition is ferromagnetic at room temperature leading to direct ferromagnetic coupling between Fe layers in $\text{Fe}/\text{Si}_{40}\text{Fe}_{60}$ multilayers (Fig. 1a). The strongest antiferromagnetic coupling $J=-1.94 \text{ mJ/m}^2$ accompanied by saturation field of $H_S=1.51 \text{ T}$ has been found for Fe/Si multilayers with $d_{\text{Si}}=1.4 \text{ nm}$. We have found (Fig.1a) that both saturation field and so-called F_{AF} parameter ($F_{\text{AF}}=1-M_{\text{R}}/M_{\text{S}}$, where M_{R} and M_{S} denote remanent and saturation magnetizations, respectively) decline when x decreases. Figure 1b shows that for all examined $\text{Fe}/\text{Si}_x\text{Fe}_{1-x}$ multilayers (except $\text{Fe}/\text{Si}_{40}\text{Fe}_{60}$ MLs) only a single saturation field maximum versus spacer layer thickness has been observed however, its position moved toward the thicker spacer layer with decreasing x . Above the $H_S(d_S)$ maximum for thicker spacer layer its values was found to decay exponentially. The reduction of F_{AF} parameter (F_{AF} indicates fraction of the ML which is antiferromagnetically



coupled) and H_S values below the $H_S(d_S)$ maximum points out that the neighboring Fe layers become gradually connected through pinholes. It was confirmed by F_{AF} and H_S temperature measurements which showed that $F_{AF}(T)$, of the samples with d_S representing H_S maximum, always decreases with decreasing temperature in spite of continuous $H_S(T)$ improvement.

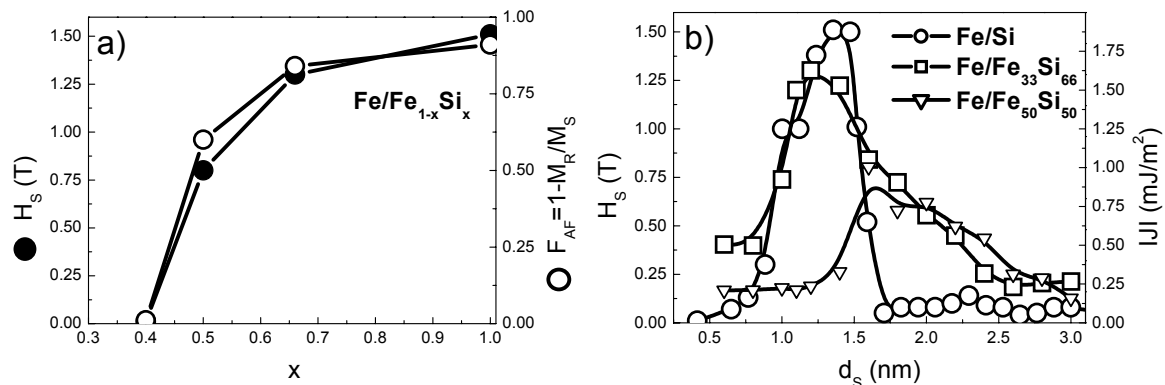


Figure 1. Spacer layer composition dependence of the saturation field H_S and F_{AF} parameter (a), and the values of H_S and coupling energy J versus spacer layer thickness d_S for different x in Fe/Si_xFe_{1-x} multilayers (b).

Above results may suggest that the appearance of the observed H_S maximum versus spacer layer thickness is not due to RKKY-like coupling mechanism. The observed non-oscillatory but exponentially decaying saturation field values seems to correspond rather to the quantum interference model of exchange coupling [6]. Comparing the results obtained for Fe/Si , $Fe/Si_{66}Fe_{33}$ and $Fe/Si_{50}Fe_{50}$ multilayers we may conclude that for certain d_S range the Si , $Si_{66}Fe_{33}$ and $Si_{50}Fe_{50}$ spacer layers mediate antiferromagnetic coupling in $(Fe/Si_xFe_{1-x})_{15}$ multilayers however, the coupling energy is distinctly stronger for nominally pure Si spacer layer.

Supported by the State Committee for Scientific Research under grants PBZ/KBN-013/T08/23 and PBZ/KBN/044/PO3/2001.

- [1] R. R. Gareev, D. E. Buegler, M. Buchmeyer, R. Schreiber, and P. Gruenberg, *J. Magn. Magn. Mater.* **240**, 235 (2002)
- [2] S. Toscano, B. Briner, H. Hopster, M. Landolt, *J. Magn. Magn. Mater.* **114**, L6 (1992)
- [3] M. Xiao, Z. Li, *Phys. Rev. B* **54**, 3322 (1996)
- [4] E. F. Fullerton, S. D. Bader, *Phys. Rev. B* **53**, 5112 (1996)
- [5] K. Inomata, K. Yusu, Y. Saito, *Phys. Rev. Lett.* **74**, 1863 (1995)
- [6] P. Bruno, *J. Appl. Phys.* **76** 6972 (1994)



**INTERFACE-LOCALIZED MODE AND CRITICAL ANGLE EFFECT
IN FMR SPECTRUM OF EXCHANGE-COUPLED BILAYER FILMS**

S. MAMICA and H. PUSZKARSKI

Surface Physics Division, Faculty of Physics, Adam Mickiewicz
University, 61-614 Poznań, Umultowska 85, Poland

From the experimental viewpoint, a characteristic feature of ferromagnetic resonance (FMR) in bilayer films is that some specimens show single resonance, whereas others show double resonance. Double resonance can exhibit a regular pattern in which the high-field (HF) line intensity surpasses that of the low-field (LF) line, or it can exhibit an *inverted* pattern with the HF line less intense than the LF line. There is a general agreement that the inverted FMR pattern occurs when the HF line is an '*optic mode*', *i.e.* an out-of-phase composition of individual sublayer modes, and the LF line is an '*acoustic mode*', or an in-phase mode composition. The existing theoretical explanations of bilayer ferromagnetic resonance are, as a rule, based on phenomenological equation of motion of the magnetization. In this work, we propose a theory of FMR in bilayer film based on an entirely microscopic approach, using the Heisenberg model of localized spins and assuming that the two ferromagnetic sublayers are exchange-coupled through their interface; both the strength and the sign of this interface coupling (J_{int}) is arbitrary (we admit ferromagnetic or antiferromagnetic interface coupling). The Hamiltonian contains an exchange energy and a Zeeman energy terms; the external field is assumed to be applied obliquely to the film surface. We focus on the effects originating in the interface coupling, though the system is assumed to exhibit also *pinning* effects originating from surface anisotropy on the outer surfaces of the film as well as from intrinsic interface anisotropy present on internal interfaces. The latter is assumed to consist of two components, corresponding to uni-directional (K_{int}) and uni-axial (D_{int}) anisotropies. We show that the resonance spectrum in symmetric bilayer is completely independent of J_{int} , but depends strongly on the applied static field configuration with respect to the interface normal (angle θ). A critical angle θ_{crit} is found to exist (as in the case of single-layer film) for which the multipeak spectrum reduces to a single-peak spectrum. By applying this rigorous microscopic FMR theory we do show that the inverted pattern of the bilayer FMR spectrum can also be explained if the HF line is assumed to correspond to an *in-phase mode*, *but of interface-localized nature*. Then, its intensity decreases with growing strength of its localization on the interface and, when the localization becomes sufficiently strong, the intensity of the localized mode becomes lower than that of the other mode (which is of the bulk type). This gives a possibility to explore the HF resonance line corresponding to the interface-localized mode as a potential source of information concerning the bilayer interface.



THEORY OF MAGNETOSTATIC MODES IN THIN PLATES

M. Krawczyk¹, H. Puszkarski¹, S. Mamica¹ and J.-C.S. Lévy²

¹Surface Physics Division, Faculty of Physics, A. Mickiewicz University,
ul. Umultowska 85, 61-614 Poznan, Poland;

²LPTMC, case 7020, EA 2382 and Pôle MPQ FDR CNRS 2437, Université Paris 7 Denis
Diderot, 2 Place Jussieu, 75251 Paris cedex 05, France.

The dipolar field static and dynamic components are calculated in thin plates in saturating field applied parallel or perpendicularly to the sample surface. Lattice sums, a generalization of the sums used in theoretical treatment of infinite samples with short-range interactions, are calculated numerically, and found to be in good agreement with our analytical approximations proposed for a confined system. The equations of motion are derived for a system with pure dipolar interactions, and magnetostatic modes propagating perpendicularly to the sample surfaces are calculated. The corresponding frequency spectra and mode profiles are computed numerically with emphasis laid on size effects. The lowest-frequency modes, exhibiting typical antiferromagnetic profile, are identified as surface-localized modes. The profiles of the highest-frequency modes are found to be close to the uniform mode profile.

These results are compared with available recent experimental ferromagnetic measurements [1,2] reporting the observation of resonance spectra with well-resolved magnetostatic modes. Consequences for the magnetic reversal dynamics will be discussed as well.

[1] M. Pardavi-Horvath *et al.* J. Appl. Phys. **87** (2000) 4969.

[2] S. Tamaru *et al.* J. Appl. Phys. **91** (2002) 8034.



Centre of Excellence: Magnetic and Molecular Materials for Future Electronics

Institute of Molecular Physics, Polish Academy of Sciences
ul. Mariana Smoluchowskiego 17, 60-179 Poznań, Poland

**HALF-METALLIC ZINC-BLENDE COMPOUNDS AND MULTILAYERS WITH
SEMICONDUCTORS**

Ph. Mavropoulos, I. Galanakis, and P.H. Dederichs

IFF, Forschungszentrum Juelich, D-52425 Juelich, Germany

Zinc-blende compounds of transition elements with group-V and VI elements, such as CrAs, have been reported to be half-metallic with high Curie temperature. They represent the concentrated limit of magnetic semiconductors. The fabrication of such materials and their multilayers with semiconductors has also been reported [1]. In a recent paper [2] we made an extensive theoretical study of the bulk of such materials and found that the half-metallic property depends on the lattice constant. We have identified systems which have equilibrium lattice constants close to the ones of semiconductors, and which are also half-metallic in these lattice constants. In this way we propose possible half-metal semiconductor combinations for coherent growth with small lattice mismatch. These are VAs/GaAs, VSb/InAs, VSb/GaSb, CrAs/GaAs, CrSb/InAs, CrSb/GaSb, MnSb/GaSb. We also extend our calculations to the case of the (001) multilayers CrAs/GaAs, CrSb/InAs, CrAs/ZnSe and CrSb/ZnTe. We find that half-metallicity can be preserved throughout the multilayers.

References

- [1] H. Akinaga *et al.*, Jpn. J. Appl. Phys. **39**, L1118 (2000); M. Mizuguchi *et al.*, J. Magn. Magn. Mater. **239**, 269 (2002).
- [2] I. Galanakis and Ph. Mavropoulos, Phys. Rev. B **67**, 104417 (2003).



**ELECTRONIC STRUCTURE, MAGNETISM AND HYPERFINE PARAMETERS OF
Fe_{3-x}Ti_xAl (0 ≤ x ≤ 1) ALLOYS**

T. Michalecki, J. Deniszczak, J.E. Frąckowiak

Institute of Physics and Chemistry of Metals, University of Silesia
40-007 Katowice, Bankowa 12, Poland

In the last decade several representatives of the ternary transition metal intermetallics with the Heusler-type crystal structure have been widely investigated with the aim of explaining the origin of their anomalous heavy-fermion-like behavior. It was discovered that in Heusler compounds Fe_{2+x}V_{1-x}M (M=Al, Ga, Si) the semiconductor-like resistivity behavior accompanies the large value of the low temperature electronic specific coefficient γ and the presence of the clear Fermi cutoff in the XPS spectra [1,2]. We did not find detailed information on the properties of Fe_{2+x}Ti_{1-x}Al while the much less anomalous resistivity behavior has been reported for Fe_{2+x}Ti_{1-x}M (M=Ga, Si) [2].

Electronic structure calculations for Fe_{2+x}V_{1-x}M (M=Al, Ga) with low concentration of anti-site defects (Fe at V position — $x=0.06, 0.12$, and V at Fe position — $x=-0.06$) have shown that the both types of the anti-site defects give rise to the narrow bands (of d character) located near the Fermi energy (where in the stoichiometric Heusler Fe₂VM compounds the quasi gap forms) which may response for the anomalous properties of these compounds [3,4].

The aim of the presented study was to investigate an effect of the alloying on the electronic structure, magnetic and hyperfine properties of Heusler type Fe_{3-x}Ti_xAl alloys. The band structure calculations were performed with the use of the tight-binding linearised muffin tin orbital method in the spin-polarised mode (the spin-orbit interaction was not taken into account). The calculations predict the magnetic ground-state of the Heusler Fe₂TiAl with the half-metallic density of states (DOS) in the vicinity of Fermi level (ϵ_F). As Fig. 1 shows, the DOS near ϵ_F has the quasi-gap in the majority spin channel. The minority spin DOS quasi-gap is shifted above ϵ_F . For the purpose of the alloying simulations we have performed the calculations with the use of the super-cell including eight formula units. For Ti concentrations $x=0, 0.25, 0.5, 0.625, 0.75, 0.875, 1$ different configurations of the Fe atoms were tested and the site preference have been established. For each preferred energetically configuration the volume optimization have been done. Figure 2 presents the concentration dependence of the average hyperfine field ($\langle B_{hf} \rangle$) and related total magnetic moment (per formula unit). The magnetic moment is on the decrease with concentration similar to $\langle B_{hf} \rangle$. The strong magnetic moment for Heusler concentration Fe₂TiAl is carried by iron atoms.



The calculated hyperfine parameters and their concentration dependence are in good agreement with that resulted from the Moessbauer spectroscopy [5].

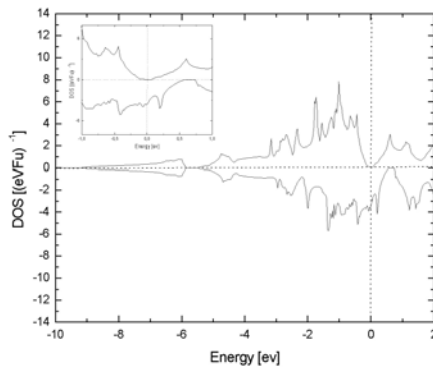


Fig. 1 Total DOS in Fe₂TiAl obtained from TB-LMTO calculation. In the insert the total DOS in the vicinity of E_F is

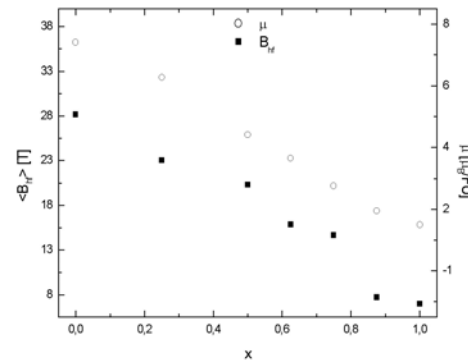


Fig. 2 Total magnetic moment and the average hyperfine field on Ti concentration (x) for Fe_{3-x}Ti_xAl

References

- [1] M. Kato, Y. Nishino, U. Mizutani, S. Asano, J. Phys.: Condens Matter, **12**, 1769 (2000).
- [2] W. Zarek, E. Talik, J. Heimann, M. Kulpa, A. Winiarska, M. Neumann, J. Alloys Comp., **297**, 53 (2000), and references therein.
- [3] J. Deniszczuk, Acta Phys. Pol., **B32**, 529 (2001),
- [4] J. Deniszczuk, W. Borgieł, phys. stat. sol. (a) **196**, 236-239 (2003).
- [5] K. Brząkalik, J.E Frąckowiak, Nukleonika (2003) in press



**XPS SPECTRA, ELECTRONIC STRUCTURE AND ELECTRICAL RESISTIVITY
OF YNi₄B COMPOUND**

M. Pugaczowa-Michalska^{1,*}, G. Chelkowska², T. Toliński¹ and A. Kowalczyk¹

¹*Institute of Molecular Physics, Polish Academy of Sciences,
Smoluchowskiego 17, 60-179 Poznań, Poland*

²*Institute of Physics, Silesian University, Uniwersytecka 4, 40-007 Katowice, Poland*

The electronic structure of the ternary YNi₄B compound, crystallizing in the hexagonal CeCo₄B structure (P6/mmm space group), was studied by X-ray photoelectron spectroscopy (XPS) and ab-initio calculations. Core levels and the valence band were investigated. The XPS valence band is compared with that obtained from ab-initio calculations. The valence band spectrum at the Fermi level exhibits the domination of the Ni(3d) states, which are hybridized with 4d states of Y and 2p states of B. The total, partial density of states of YNi₄B, obtained from electronic structure calculations, reveal the hybridisation d states of Ni with d-states of Y and p-states of B. The self-consistent electronic structure calculations were performed for the experimental lattice constant and for the lattice parameter estimated from the minimum of the total energy. The equilibrium lattice parameters are $a=5.143 \text{ \AA}$ and $c=7.165 \text{ \AA}$. The theoretical values of lattice parameters are about 3.13% higher than the experimental ones. The calculated electronic specific heat coefficient γ derived from $N(E_F)$ is about $11.33 \text{ mJ/mol}\cdot\text{K}^2$ for experimental lattice parameters. The calculated bulk modulus is $B_0=1.61632 \text{ Mbar}$. The temperature dependence of electrical resistivity can be described using the modified Bloch-Grüneisen relation. The $\rho(T)$ curve above the transition temperature can be well fitted using the modified Bloch-Grüneisen relation. The experimental Debye temperature Θ_D is 240 K is in good agreement with calculated value ($\Theta_D=273 \text{ K}$).



**CRYSTALLOCHEMICAL AND MAGNETIC BEHAVIOUR OF $\text{Sc}(\text{FeAl})_{12}$ SAMPLES
BY POWDER DIFFRACTION AND MOESSBAUER TECHNIQUES**

K. Rećko^a, K. Szymański^a, L. Dobrzyński^{a,b}, D. Satuła^a and B.C. Hauback^c, W. Suski^{d,e},
B. Yu. Kotur^f

^a Institute of Experimental Physics, Univ. of Białystok, Lipowa 41, 15-424 Białystok, Poland

^b The Soltan Institute for Nuclear Studies, 05-400 Otwock-Świerk, Poland

^c Dept. of Physics, Institute for Energy Technology, P.O. Box 40, N-2027 Kjeller, Norway

^d W. Trzebiatowski Institute of Low Temperature and Structure Research, PAS,

P.O. Box 1410, 50-950 Wrocław 2, Poland

^e International Lab. of High Magnetic Fields and Low Temperatures,

ul. Gajowicka 95, 53-421 Wrocław, Poland

^f Department of Inorganic Chemistry, L'viv State University,

bul. Kirila i Mefodiya 6, L'viv 290005, Ukraine

Chemical ordering and magnetic properties of ScFe_4Al_8 , ScFe_5Al_7 and ScFe_6Al_6 powder samples are presented. These alloys have been measured by means of powder diffraction techniques, namely X-ray and thermal neutron one, conventional Moessbauer effect (ME) method as well as by Monochromatic Circularly Polarized Moessbauer Source (MCPMS). X-ray and neutron powder patterns allowed to determine crystallochemical structure of $\text{Sc}(\text{FeAl})_{12}$ alloys with symmetry $I4mmm$, isostructural with ThMn_{12} – type of structure. Our earlier studies carried out on crystal and magnetic structures of $(\text{U}, \text{Th})(\text{FeAl})_{12}$ intermetallic compounds [1-2] indicated large crystallochemical similarity in both series of actinide's alloys. In the case of scandium samples this rule was broken. The latter turned out to exhibit new type of precipitations appearing during annealing procedure as well as a new kind of disordering within their lattices. In the case of scandium alloys the extra phases disclosed much lower symmetry than the ones, mainly cubic FeAl -type, appearing in U- or Th-samples. In addition, the a-f disordering in the basic phase was observed which contrasts with previously investigated samples where typically f-j disordering took place.

On the magnetic side, with increasing iron content the isostructural $\text{UFe}_x\text{Al}_{12-x}$ alloys [1-2] exhibited the transition from spin-canted system for $x=4$, with the antiferromagnetic interactions as a dominant ones, to the ferromagnetic ordering for $x=6$. In the case of ThFe_4Al_8 sample in which only iron atoms were responsible for magnetism, the incommensurate magnetic structure was discovered [3]. The same situation was found in scandium sample with $x=4$. We note that the magnetic behaviour of ScFe_4Al_8 raised already some controversies in the literature [4-5]. The published results indicated presence of a spin glass state or a mixture of antiferromagnetic structure and spin glass. Our unpolarized neutron diffraction pattern, however, leaves no doubts that the modulated magnetic structure is



observed in the ScFe_4Al_8 compound. The interpretation of the neutron data requires presence of non-zero magnetic propagation vector different from the nuclear one. The iron magnetic moments of ScFe_4Al_8 sample create spiral structure with spins rotated in a plane parallel to the wave vector $q=(q_x, q_x, 0)$, with $q_x = 0.136(2)$ which is temperature independent up to 175 K. The value of iron magnetic moment at 8 K is close to $1.08(12) \mu_B$. The basic magnetic cell has to be purely antiferromagnetic with iron spins directed along **a** or **b** axis and rotated in the basal plane by $49(1)^\circ$ from cell to cell. The antiferromagnetic nature of ScFe_4Al_8 is fully confirmed by Moessbauer measurements. All Moessbauer spectra were measured at the magnetic field of 1 T. The magnetic spectra's components in the ME and MCPMS diagrams show that the angular distribution of iron magnetic moments is independent of the external magnetic field. This is typical for antiferromagnetically ordered sample. In contrast to that, the MCPMS spectra measured for ScFe_6Al_6 show that the angular distribution of iron magnetic moments is strongly dependent on the magnetic field that proves in turn a ferromagnetic nature of this alloy. The hyperfine magnetic field of ScFe_4Al_8 is equal to 11.20(2) T, very close to 11.5(3) T and 11.0(2) T obtained for ThFe_4Al_8 [3] and UFe_4Al_8 [1-2], respectively. The iron magnetic moment in the 1 T field reaches value of $1.24(8) \mu_B$ at 12 K.

Because neither scandium nor thorium bear magnetic moments in the samples of our interest, the iron atoms must play key role in formation of the incommensurate magnetic structures in both, scandium and thorium alloys. In the case of uranium samples, the uranium itself is active ion formation of the magnetic structure, so one faces the necessity of explanation of all additional magnetic interactions, including anisotropic ones.

References

- [1] K. Rećko, K. Szymański, L. Dobrzyński, J. Waliszewski, D. Satuła, M. Biernacka, K. Perzyńska, W. Suski, K. Wochowski, A. Hoser, G. André, F. Bourée, *J. Alloys Comp.* **323-324** (2001) 531
- [2] K. Rećko, K. Szymański, L. Dobrzyński, D. Satuła, W. Suski, K. Wochowski, G. André, F. Bourée, A. Hoser, *J. Alloys Comp.* **334** 1-2 (2002) 58
- [3] K. Rećko, L. Dobrzyński, K. Szymański, D. Satuła, K. Perzyńska, M. Biernacka, J. Waliszewski, P. Zaleski, W. Suski, K. Wochowski, M. Hofmann and D. Hohlwein, *Phys. Stat. Sol. (a)* **196** (2003) 344
- [4] B.Yu. Kotur, D. Badurski, W. Suski, K. Wochowski, A. Gilewski, T. Mydlarz, *Physica B* **254** (1998) 107
- [5] P. Gaczyński, F.G. Vagizov, W. Suski, B.Yu. Kotur, W. Iwasieczko, H. Drulis, *J. Magn. Magn. Mater.* **225** (2001) 351



XPS STUDIES OF NANOCRYSTALLINE AND POLYCRYSTALLINE LaNi_5 THIN FILMS

L. Smardz¹, K. Smardz², M. Nowak², M. Jurczyk²

¹Inst. of Molecular Phys., Polish Acad. of Sci., Smoluchowskiego 17, 60-179 Poznań, Poland

²Inst. of Materials Sciences and Engineering, Poznań Univ. of Technology, M. Curie 5 Sq., Poznań, Poland

A large number of experimental investigation on LaNi_5 and related compounds have been performed up to now in relation to their exceptional hydrogenation properties [1]. In order to optimise the choice of the intermetallic compounds for a selected application, a better understanding of the role of each alloy constituent on the electronic properties of the material is crucial. Several semi-empirical models [2, 3] have been proposed for the heat of formation and heat of solution of metal hydrides and attempts have been made for justifying the maximum hydrogen absorption capacity of the metallic matrices. These models showed that the energy of the metal - hydrogen interaction depend both on geometric and electronic factors. In this contribution, we study experimentally the electronic properties of polycrystalline and nanocrystalline LaNi_5 thin films using X-ray photoelectron spectroscopy (XPS). For a comparison we will also show XPS results for bulk nanocrystalline and polycrystalline $\text{LaNi}_{4.2}\text{Al}_{0.8}$ alloys. The structure of the samples has been studied by X-ray diffraction (XRD). Their bulk chemical compositions were measured using X-ray fluorescence (XRF) method. The scanning electron microscopy (SEM) technique was used to follow the changes in size and shape of the grains. These measurements may supply useful indirect information about the influence of the electronic structure of polycrystalline and nanocrystalline LaNi_5 -type alloys on their hydrogenation properties.

LaNi_5 alloy thin films were prepared onto glass substrates in the temperature range 285 – 700 K using computer-controlled ultra high vacuum (UHV) magnetron co-sputtering. Ni and La targets were sputtered using DC and RF modes, respectively. The base pressure before the deposition process was lower than 5×10^{-10} mbar. The chemical composition and the cleanness of all layers was checked *in-situ*, immediately after deposition, transferring the samples to an UHV (4×10^{-11} mbar) analysis chamber equipped with XPS [4]. The XPS spectra were measured with Al-K_α radiation at 1486.6 eV at room temperature using a SPECS EA 10 PLUS energy spectrometer. All emission spectra were measured immediately after sample transfer in a vacuum of 8×10^{-11} mbar. The deposition rates of La and Ni and LaNi_5 thin films are individually checked by a quartz thickness monitors. Typical deposition rate of LaNi_5 thin films was about 0.15 nm/s. The thickness and composition of the deposited films were also determined using X-ray fluorescence analysis (XRF).

The polycrystalline $\text{LaNi}_{4.2}\text{Al}_{0.8}$ alloy was prepared by arc melting stoichiometric amounts of the constituent elements (purity 99.9% or better) in a high purity argon atmosphere. The as cast ingot was homogenised at 1170 K for 3 days and then rapidly cooled to room temperature in water. The average grain size of the polycrystalline sample was about 500 nm.

The nanocrystalline $\text{LaNi}_{4.2}\text{Al}_{0.8}$ alloy was prepared using mechanical alloying (MA) followed by annealing. MA was performed under argon atmosphere using a SPEX 8000 Mixer Mill. Results show that the amorphous phase of MA samples forms directly from the starting mixture of the elements, without other phase formation. Heating the MA powders at 1070 K for 1 h resulted in the creation of hexagonal CaCu_5 -type nanocrystalline compound with mean crystallite size less than 50 nm.



Structural studies showed that the LaNi_5 thin films deposited at 295 K are nanocrystalline with average grain size $D \sim 15$ nm. Thin films deposited at about 700K are polycrystalline with $D \sim 200$ nm. The total thickness of the samples was about 1000 nm.

In Fig. 1 we show the XPS valence bands for nanocrystalline (bold solid line) and polycrystalline (thin solid line) LaNi_5 films. The shape of the valence band measured for the polycrystalline LaNi_5 thin film is practically the same compared to that reported earlier for the single crystalline sample [1]. On the other hand, the XPS valence band of the nanocrystalline LaNi_5 thin film (bold solid line) is considerably broader compared to that measured for the polycrystalline sample. This is probably due to a strong deformation of the nanocrystals. Normally the interior of the nanocrystal is constrained and the distances between atoms located at the grain boundaries expanded. Similar broadening of the valence band can be also observed for the MA nanocrystalline $\text{LaNi}_{4.2}\text{Al}_{0.8}$ bulk alloy (bold broken line) compared to that measured for the polycrystalline bulk sample (thin broken line).

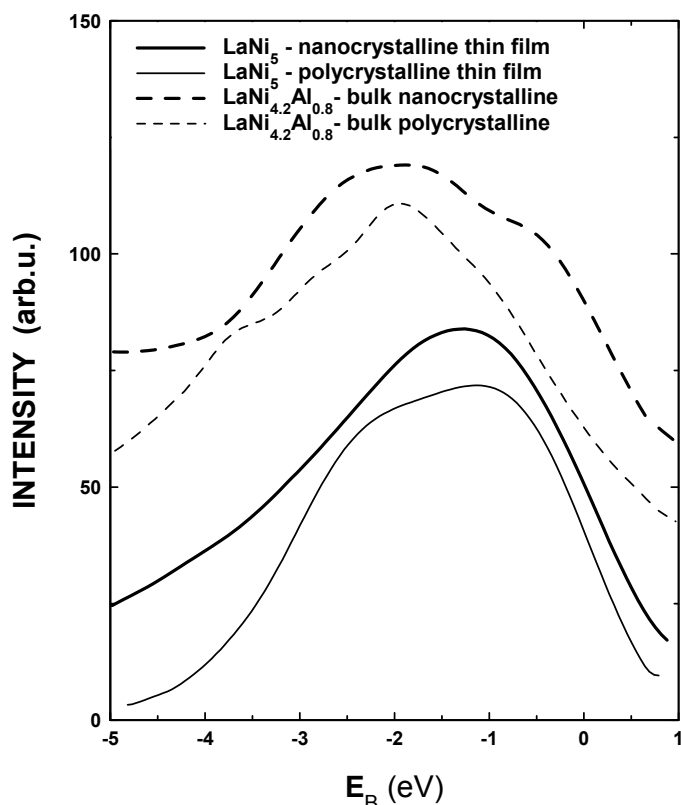


Fig.1. XPS valence band spectra for nanocrystalline (bold solid line) and polycrystalline (thin solid line) LaNi_5 thin films using $\text{Al-K}\alpha$ radiation. For a comparison we show results for the nanocrystalline and polycrystalline $\text{LaNi}_{4.2}\text{Al}_{0.8}$ bulk alloys represented by bold and thin broken lines, respectively. The spectra of the thin films were measured *in-situ*, immediately after deposition. The bulk samples were measured immediately after heating in UHV conditions followed by removing of a native oxide and possible impurities layer using ion gun etching system.

In conclusion, the different microstructure observed in polycrystalline and nanocrystalline LaNi_5 - type alloys prepared as a bulk material or thin film leads to significant modifications of the electronic structure of the intermetallic. Such a modification of the electronic structure of the nanocrystalline LaNi_5 - type alloy compared to that of polycrystalline sample could significantly influence on its hydrogenation properties [4].

This work was supported by the KBN grant No PBZ-KBN-013/T08/02.

REFERENCES

- [1] L. Schlapbach, Hydrogen in Intermetallic Compounds, II, Springer, Berlin, 1992, p. 165
- [2] P. C. Bouten, A. R. Miedema, J. Less Common Metals, 71 (1980) 147-160.
- [3] R. Griessen, Phys. Rev. B38 (1988) 3690-8.
- [4] L. Smardz, K. Smardz, M. Jurczyk, J. Jakubowicz, J. Alloy Comp. 313 (2000) 192-200.



**0.7 ANOMALY IN QUANTUM POINT CONTACT, MODELLING BASED ON
ANDERSON MODEL**

Piotr Stefański and Bogdan R. Bułka

Institute of Molecular Physics of the Polish Academy of Sciences
ul. Smoluchowskiego 17, 60-179 Poznań, Poland

An unusual temperature behavior of the conductance vs. gate voltage in quantum point contact (QPC) has been observed for years [1, 2] without satisfactory theoretical explanation. Recently it has attracted large interest again and there are strong evidences for the Kondo effect to be responsible for it [3, 4].

We model a QPC by localized spin-degenerate quasi-bound state (QBS) located inside the constriction which forms QPC. Electrons occupying QBS interact with the strength of Coulomb repulsion U , and QBS is hybridized with electrodes (2D-electron baths). Such a system we describe in the frame of the Anderson Hamiltonian:

$$H = \sum_{k,\sigma,\alpha=L,R} \varepsilon_{k,\alpha} c_{k\sigma,\alpha}^+ c_{k\sigma,\alpha} + \sum_{\sigma} \varepsilon_d d_{\sigma}^+ d_{\sigma} + U n_{\uparrow} n_{\downarrow} + \sum_{k,\sigma,\alpha=L,R} \nu_{\alpha} [c_{k\sigma,\alpha}^+ d_{\sigma} + d_{\sigma}^+ c_{k\sigma,\alpha}].$$

The hybridization $\Gamma = \pi \nu^2 \rho_{el,\alpha}$ ($\rho_{el,\alpha}$ is the density of states in the α -electrode) is assumed to have a step-like profile to simulate the potential barrier present inside QPC and increasing transparency of the QPC when the potential of the confining gate increases and the QBS level approaches Fermi surface.

Firstly, the non-interacting case is analyzed. Without interactions the Hamiltonian is quadratic in operators and can be solved exactly. The step-like behavior of the experimental first plateau in conductance is reproduced. The hybridization of the bound state with electrodes for the fully transparent QPC is one order of magnitude larger comparing to quantum dots.

Interacting case is analyzed within the Interpolative Perturbative Scheme (IPS) [5] which is an extension of the second order perturbation in U to the atomic limit [6]. We have modified the method to be applicable for the case when the hybridization increases in the step-like fashion. The method is applied both for strong (Kondo regime) and weak (Coulomb



blockade regime) hybridization. Such crossover from one regime to another indeed takes place in QPC when the hybridization of QBC with electrodes increases while increasing of the gate voltage.

We start our modeling when the bound state inside QPC is initially weakly coupled to electrodes. Even for an infinitesimally small hybridization the level is fully occupied by two electrons with opposite spins when it lies below Fermi surface at $T=0$. Then, when the bare level is shifted towards Fermi surface it enters the region where the level $\varepsilon_d+n_\sigma U$ is pushed above the Fermi level and starts to be empty. This is a regime when the conductance is mainly enhanced by the Kondo effect. Then, the occupancy of the level ε_d decreases though the hybridization with electrodes increases. Thus, the level occupancy is controlled mainly by the position of the level relative to Fermi surface.

The anomaly around the value of $0.7x$ ($2e^2/h$) appears in the conductance curves vs. QBS level position when temperature increases. The shape of the curves strongly depends on the energy for which the hybridization step takes place. The 0.7 anomaly arises as a result of the competition between two mechanisms of enhancing the conductance up to the unitary limit: the Kondo effect and the increase of hybridization.

- [1] N.K. Patel *et al.*, Phys. Rev. B44, 13549 (1991).
- [2] K.J. Thomas *et al.*, Phys. Rev. Lett. 77, 135 (1996).
- [3] S.M. Cronenwett *et al.*, Phys. Rev. Lett. 88, 226805 (2002).
- [4] Y. Meir *et al.*, Phys. Rev. Lett. 89, 196802 (2002).
- [5] A. Levy-Yeyati *et al.*, Phys. Rev. Lett. 71, (1993) 2991.
- [6] K. Yoshida *et al.*, Prog. Theor. Phys. 46, (1970) 244.



**ELECTRONIC STRUCTURE AND PHOTOEMISSION SPECTRA OF
USn₂ COMPOUND**

A. Szajek

Institute of Molecular Physics, Polish Academy of Sciences, Poznań, Poland

The *ab-initio* self-consistent calculations have been performed for USn₂ compound, which crystallizes in the ZrGa-type structure (*Cmmm* space group). The tight binding linear muffin-tin orbital method (*TB LMTO*) in the atomic sphere approximation (*ASA*) was used in the calculations. The spin-polarized calculations have confirmed the antiferromagnetic order in the USn₂ system. The magnetic moment is predominantly located on the uranium atoms and is formed mainly by the f electrons. The three types of Sn atoms may be treated as nonmagnetic. The calculated X-ray photoemission spectra are presented.

Work supported by the KBN Grant No. 2 P03B 023 22 and the Centre of Excellence for Magnetic and Molecular Materials for Future Electronics within the European Commission Contract No. G5MA-CT-2002-04049.



Centre of Excellence: Magnetic and Molecular Materials for Future Electronics

**Institute of Molecular Physics, Polish Academy of Sciences
ul. Mariana Smoluchowskiego 17, 60-179 Poznań, Poland**

MODEL OF NANOCOMPOSITE MAGNETIC GRAIN

A. Szlaferek

Institute of Molecular Physics, Polish Academy of Sciences,
Smoluchowskiego 17, 60-179 Poznań, Poland

A good permanent magnet must have a high energy product. Kneller and Hawig proposed an approach to enhance the energy product by making a nanocomposite of exchange coupled hard and soft magnetic phases. The hard phase provides the required magnetic anisotropy and stabilizes the exchange coupled soft phase against demagnetization.

In this paper present a model of nanocomposite magnetic grain. The grain consist of the shell soft magnetic spherical kernel surrounded by a spherical shell of the hard magnetic material. This grain is embedded in the soft magnetic matrix.

Calculations of the process of reversal magnetization are performed basing on the model. The kernel has the radius r_3 , possesses an easy axis in the direction of z axis. Magnetization also lies in the z direction. The spherical shell has the external radius r_2 , its magnetization and easy axis have the direction of the z axis.

The magnetization reversal of nanocomposite two-phase grains are calculated applying Brown's equation. Solutions of Brown's differential equation for the minimization of the total free energy of the spheroid are presented.

The magnetic free energy, can be written as

$$E = 2\pi \int_0^\pi \sin \theta d\theta \left(\int_0^{r_3} F_s r^2 dr + \int_{r_2}^{r_3} \left[F_h - \frac{2}{3} \pi (M_h^2 - M_s^2) \omega_2^2 \right] r^2 dr + \int_{r_2}^\infty F_s r^2 dr \right) \quad (1)$$

where the second term in the square bracket represents the demagnetizing energy density.

Here,

$$F_j = A_j \left(\left(\frac{\partial \omega}{\partial r} \right)^2 + \frac{1}{r^2} \left(\frac{\partial \omega}{\partial \theta} \right)^2 + \frac{\omega^2}{r^2 \sin^2 \theta} \right) + K_j \omega^2 - \frac{1}{2} H_a M_j \omega^2 \quad j = h, s \quad (2)$$



The first term represents a density of energy of exchange interaction, the second one - density of energy of anisotropy and the last term represents a density of energy of Zeeman interactions. M_s , M_h denote magnetization of soft and hard magnetic phases, respectively, A is the exchange constant, K uniaxial anisotropy constant and H_a is the external magnetic field. Minimizing the magnetic energy and solving it, with respect to boundary conditions at the interface, we obtain $\omega_1(t)$, $\omega_2(t)$, $\omega_3(t)$.

The state of magnetization of the whole grain is defined as the sum magnetization of its parts. These are functions of angles ω_2 and ω_3 . The numerical solution of the equations $\omega_2(t)$ and $\omega_3(t)$, provide us the direction of rotation of the magnetization in the kernel and the shell determined by the geometry of the grain and external magnetic field. We find directions of the magnetization ω_2 as a function of the reduced shell thickness and external magnetic field H_a , and directions of magnetization ω_3 as a function of the reduce kernel size and external magnetic field H_a .

With the decrease of the thickness of the shell the angle, ω_2 gets smaller. On the other hand, the increase of the external magnetic field strength also contributes to the value of the angle ω_2 . On the other hand, with increasing H_a , ω_3 increases to the value π . When H_a is small, magnetization of the soft kernel can be reversed only with difficulty and ω_3 is small. With increasing H_a , the exchange force action on magnetization of the hard phase with the magnetization of the soft phase inside becomes strong, preventing magnetization of soft kernel from reversal.



Ni/Cu/Co TRILAYERS WITH OUT-OF-PLANE Ni MAGNETIZATION: *in-situ*
MOKE INVESTIGATIONS

T. Toliński*, K. Lenz, E. Kosubek, J. Lindner, K. Baberschke

Institute fuer Experimentalphysik, Freie Universitaet Berlin,
Arnimallee 14, D-14195 Berlin-Dahlem, Germany

We have prepared Ni/Cu_x/Co/Cu(001) films in ultrahigh-vacuum (base pressure of about 5×10^{-11} mbar) with variable spacer thickness ($4\text{ML} < x < 50\text{ML}$) and constant thickness of Ni(9ML), Co(2ML) and capping Cu(4ML) layers. The films growth was monitored by MEED (medium energy electron diffraction) oscillations and the AES (Auger electron spectroscopy).

Usually trilayers characterized by in-plane or perpendicular anisotropy of *both* ferromagnetic (FM) films are studied. The thicknesses of FM films we have used lead to the exceptional case of perpendicular Ni and in-plane Co magnetization orientation, which is a result of the different out-of-plane anisotropies. Co is in-plane in the whole thickness range and Ni undergoes a transition to perpendicular direction above 7ML [1]. Additionally, this Co thickness enables room temperature studies because T_C of 2ML Co is about 340 K. Thinner Co films exhibit lower anisotropy (better for magnetic measurements), which already for 2ML is $M_{\text{eff}} = 37.6$ kG ($M_{\text{eff}} = 4\pi M - 2K_2/M$), but below 1.8ML of Co T_C jumps down to 200 K [2]. For comparison the effective magnetization of 9ML of Ni is equal to $M_{\text{eff}} = -2.18$ kG.

We have measured *in-situ* polar dc-MOKE (magneto-optical Kerr effect) hysteresis loops. The polar geometry is sensitive only to the perpendicular component of magnetization, therefore the Ni film contribution has been measured. Fig. 1 presents the calculated hysteresis loop assuming either coherent rotation of moments (solid line) or magnetization by domain wall movement (dotted line) [3,4]. The experimental loop shown in the inset is measured for an uncoupled film with a spacer thickness of 50ML. It is visible that the coercive field is strongly reduced compared to the rotational model. The domain nucleation is favoured in polar measurements, however, the coercivity is not zero, which supports the prediction that intermediate behaviour is observed [3,4].

* permanent address: Institute of Molecular Physics, PAS, Smoluchowskiego 17, 60-179 Poznań, Poland



Our investigations concern the influence of the interlayer exchange coupling on the measured polar MOKE loops with the coupling modified by changing the spacer Cu thickness. The question of the temperature dependence of the magnetization curves is also addressed. The experimental results are supported by model calculations of the hysteresis loops.

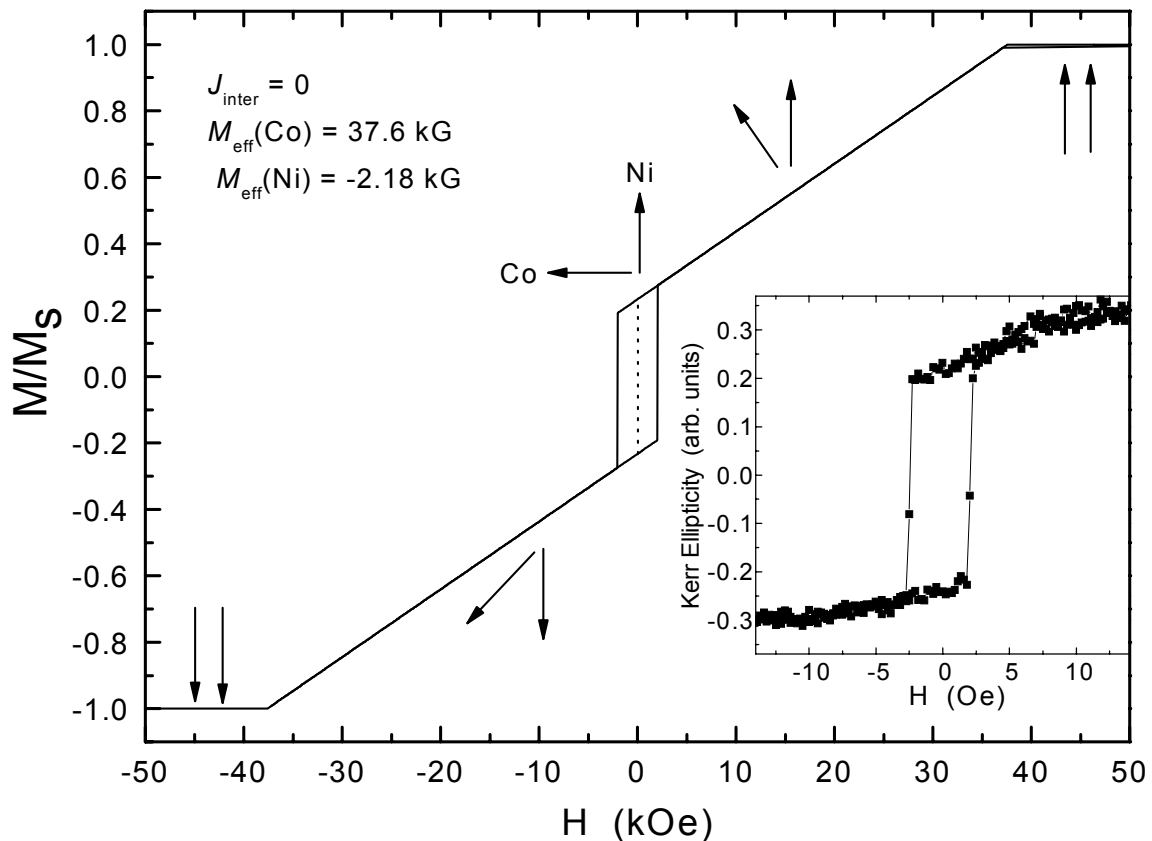


Fig. 1. Calculated magnetization curve of uncoupled $\text{Cu}_5/\text{Ni}_9/\text{Cu}_{50}/\text{Co}_2/\text{Cu}(001)$ trilayer (solid line – coherent rotation model, dotted line – domain wall movement model). Inset: Experimental polar MOKE hysteresis loop of the Ni component. One should note that the experimental coercive field is close to zero in the scale of the main figure.

References

- [1] K. Baberschke and M. Farle, *J. Appl. Phys.* **81** (1997) 5038.
- [2] P. Pouloupoulos, P.J. Jensen, A. Ney, J. Lindner and K. Baberschke, *Phys. Rev. B* **65** (2002) 064431.
- [3] B. Dieny and J.P. Gavigan, *J. Phys.: Condensed Matter* **2** (1990) 187.
- [4] T. Toliński and J. Baszyński, *phys. stat. sol. (a)* **169** (1998) 139.



**COMPARATIVE STUDIES OF STRUCTURAL, MAGNETIC AND ELECTRONIC
PROPERTIES OF NdNi₄Al AND NdNi₄B COMPOUNDS**

T. Toliński^{1}, W. Schaefer², G. Chelkowska³, W. Kockelmann⁴, A. Hoser⁵,
B. Andrzejewski¹, A. Szlaferek¹ and A. Kowalczyk¹*

¹ Institute of Molecular Physics, Polish Academy of Sciences,
M. Smoluchowskiego 17, 60-179 Poznań, Poland

² Mineralogisches Institut, Univ. Bonn, in Forschungszentrum Juelich, 52425 Juelich,
Germany

³ Institute of Physics, Silesian University, Uniwersytecka 4, 40-007 Katowice, Poland

⁴ Mineralogisches Institut, Univ. of Bonn, at ISIS Facility, Rutherford Appleton Laboratory,
Chilton OX11 0QX, U.K.

⁵ Institut fuer Kristallographie, RWTH-Aachen, Germany

We present our results on magnetic and structural studies of the hexagonal rare-earth based NdNi₄Al and NdNi₄B compounds. The samples were prepared by the induction melting of stoichiometric amounts of the constituent elements in a water-cooled boat, under an argon atmosphere. NdNi₄Al crystallizes in the hexagonal CaCu₅-type structure, space group P6/mmm, whereas NdNi₄B crystallizes in the hexagonal CeCo₄B-type structure, space group P6/mmm. The room temperature lattice constants are $a = 5.0103 \text{ \AA}$, $c = 4.0601 \text{ \AA}$ for NdNi₄Al and $a = 5.053 \text{ \AA}$, $c = 6.954 \text{ \AA}$ for NdNi₄B.

In spite of different crystallographic structures NdNi₄Al and NdNi₄B compounds exhibit many similarities in their magnetic and transport properties. The ferromagnetic ordering temperature T_C and magnetic moments at 6 T for these compounds are 6 K, $1.52 \mu_B/\text{f.u.}$ and 11.7 K, $1.68 \mu_B/\text{f.u.}$ [1], respectively. The magnetization curves are displayed in Fig. 1. The phase transitions are confirmed both by our ac/dc magnetic susceptibility (Fig.1) measurements and electrical resistivity studies [2].

* present address: Institut fuer Experimentalphysik, Freie Universitaet Berlin, Arnimallee 14, D-14195 Berlin-Dahlem, Germany



In the case of the NdNi₄Al samples we have performed also neutron diffraction studies, which are not possible for compounds containing natural boron due to large absorption. Hence, the magnetic order of NdNi₄Al has been established with the magnetic moments ordered in the hexagonal basis plane. Besides, a negligible magnetic contribution of Ni atoms was observed. This condition simplifies the interpretation of the magnetic, transport and electronic properties of RNi₄Al or RNi₄B (R = rare earth or Y) compounds.

The photoemission spectra (XPS) of the valence band region at the Fermi level exhibits the dominance of the Ni(3d) states (1.5 eV) [3].

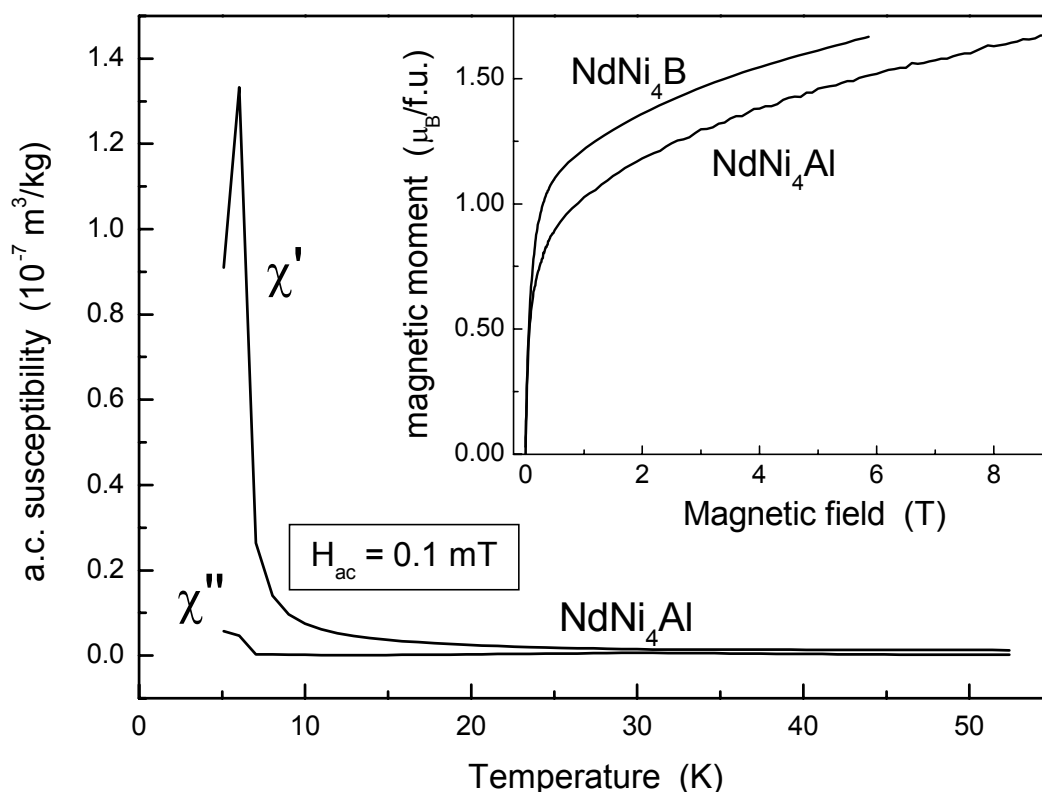


Fig. 1. The real, χ' , and the imaginary, χ'' , part of the a.c. susceptibility for NdNi₄Al compound. Inset: The magnetization curve of NdNi₄Al and NdNi₄B compounds.

References

- [1] T. Toliński, A. Kowalczyk, A. Szlaferek, M. Timko and J. Kováč,
Solid State Commun. **122** (2002) 363.
- [2] T. Toliński, A. Kowalczyk, V. Ivanov, phys. status sol. (b), accepted for publication
- [3] T. Toliński, G. Chełkowska and A. Kowalczyk, Solid State Commun. **122** (2002) 145.



KONDO EFFECT AND MIXED VALENCE IN CeNi₄X (X=B and Al) COMPOUNDS

T. Toliński^{1}, G. Chelkowska², A. Szlaferek¹, V. Ivanov³, M. Falkowski⁴ and A. Kowalczyk¹*

¹Institute of Molecular Physics PAS, Smoluchowskiego 17, 60-179 Poznań, Poland

²Institute of Physics, Silesian University, Uniwersytecka 4, 40-007 Katowice, Poland

³General Physics Institute, RAS, Vavilov 38, Moscow, Russia

⁴Faculty of Technical Physics, Poznań University of Technology, Nieszawska 13a, Poland

Despite the increased interest in the metallic systems with electronic instability of 4f-states known as systems with intermediate valence, heavy fermions or Kondo-lattices, the nature of 4f-states of Ce in the considered phases is still unclear at the microscopic level. In the Ce-based compounds, depending on the position of the Fermi level E_F compared to that of the 4f state the following electronic states of cerium are expected: magnetic 3+ state, 3+ state with Kondo effect and intermediate (3+/4+) valence state. The cerium-transition metal compounds are attractive for studies of these diverse Ce states because of the strong dependence of the Fermi level position on the amount of the contributing elements. The behavior of Ce changes in various Ce-Ni systems also due to the different crystallographic structures.

The series RNi₄B, where R stands for rare-earth element or Y is attracting attention developed owing to its interesting magnetic, structural and electronic behavior. The materials belonging to the RNi₄B series create a hexagonal structure of CeCo₄B with space group $P6/mmm$. The Ni atoms occupy the crystallographic sites (2c) and (6c), rare earth is also located in two sites (1a) (1b) and boron atoms are located in the (2d) positions. For comparison, in the case of RNi₄Al compounds (CaCu₅ –type structure) R occupies the 1a site and Ni (1) the 2c site. Ni(2) and Al are statistically distributed on the 3g site.

The X-ray photoemission spectra were obtained for the radiation of the photon energy equal to 1487.6 eV, Al-K α source using a PHI 5700/660 Physical Electronics Spectrometer. The energy spectra of the electrons were analyzed by a hemispherical mirror analyzer with the energy resolution of about 0.3 eV. The Fermi level $E_F = 0$ was referred to the gold 4f-level binding energy at 84 eV. All photoemission spectra were measured immediately after breaking the sample in a vacuum of 10^{-10} Torr.

X-ray photoelectron spectroscopy is not an ideal tool to probe the Ce 4f valence bands because of relatively small cross sections. The XPS spectra of the 3d core levels give more information about the 4f configuration and hybridization. The Ce-based intermetallic compounds show different final states depending on the occupation of the f shell: f^0 , f^1 and f^2 [1]. The spin-orbit coupling $\Delta = (3d^9 4f^1)_{3/2} - (3d^9 4f^1)_{5/2} = 18.4$ eV for CeNi₄B and CeNi₄Al. The appearance of the f^0 components is a clear evidence of a mixed valence. In α -Ce there is also evidence of the $3d^9 4f^0$ peaks for both $3d_{3/2}$ and $3d_{5/2}$ multiplets, which are not present in γ -Ce [2], however, the $3d_{5/2} f^0$ peak overlaps with the $3d_{3/2} f^2$ peak and only the $3d_{3/2} f^0$ peak can be accurately estimated [2]. The f-occupation in the initial state of α -Ce is connected with the intensity of the $3d^9 f^0$ satellite. The XPS of Ce(3d) spectra are usually interpreted in terms of

* present address: Institut fuer Experimentalphysik, Freie Universitaet Berlin, Arnimallee 14, D-14195 Berlin-Dahlem, Germany



the Gunnarsson-Schoenhammer theory [1]. Based on this model the intensity ratio $r = I(f^0)/(I(f^0) + I(f^1) + I(f^2))$ is directly related to the f-occupation. The separation of the overlapping peaks in the Ce(3d) XPS spectra was made basing on the Doniach-Šunjić theory [3]. The hybridization energy $\Delta = \pi V \rho_{\max}$ describes the hybridization part of the Anderson impurity Hamiltonian, where ρ_{\max} is the maximum DOS and V is the hybridization matrix element. Assuming the dependence of the intensity ratio r on the Δ parameter like in the case of Ce [1, 2] the Δ value is about 85 meV for 3d_{3/2} band and the f occupancy, $n_f \approx 0.83$ [4]. The hybridization for α -Ce estimated by this way from XPS 3d spectra is $\Delta = 60$ meV. For Ce intermetallic compounds with strong f shell instabilities Δ is of the order of 150 meV [1, 2].

The effective magnetic moment derived from the Curie constant C is lower than the magnetic moment of free Ce³⁺ ion ($\approx 2.4 \mu_B$). Since the magnetic moment of Ce⁴⁺ is zero, the reduction of the moment in CeNi₄B and CeNi₄Al may be due to the intermediate or fluctuating Ce valence state.

The magnetic contribution $\rho_{\text{mag}}(T)$ of the CeNi₄B [5] and CeNi₄Al resistivity was obtained by subtracting the temperature dependent part of $\rho(T)$ for the non-f-electron reference compound YNi₄X (X=B, Al) [5]. Below 15 K a shallow minimum typical of the Kondo systems is observed for CeNi₄B. At low temperature ($T < 12$ K) $\rho_{\text{mag}}(T)$ was analyzed in terms of the Kondo theory and the data were fitted with the standard formula:

$$\rho_{\text{mag}}(T) = \rho_0^\infty - \rho_K \ln T \quad (1)$$

yielding a value of $\rho_0^\infty = 88.4 \mu\Omega\text{cm}$ for the spin disorder resistivity and $\rho_K = 0.29 \mu\Omega\text{cm}$ for the Kondo coefficient. The value of the later confirms that this effect is very small. The minimum may also be induced by a Kondo-like effect originating from the intermediate or fluctuating Ce valence state.

Summarizing the results, one may conclude both from the susceptibility measurements and the XPS spectra that Ce ions in CeNi₄B and CeNi₄Al are in the intermediate valence state. These compounds are paramagnetic and follow the Curie-Weiss law. However, the derived effective magnetic moment is much lower in comparison with free Ce³⁺ ions value equal to $2.54 \mu_B$. Since magnetic moment of tetravalent cerium is zero, the observed reduction of the magnetic moment can be explained in a natural way by contribution of both the 4f⁰ (Ce⁴⁺) and 4f¹ (Ce³⁺) configurations.

The magnetic contribution to the electrical resistivity reveals in the paramagnetic region at low temperatures (below 12 K) a logarithmic slope characteristic of the Kondo-like systems.

- [1] O. Gunnarsson, K. Schoenhammer, Phys. Rev B **28** (1983) 4315.
- [2] J.C. Fuggle, F.U. Hillebrecht, Z. Zolnierok, R. Laesser, Ch. Freiburg, O. Gunnarsson, K. Schoenhammer, Phys. Rev. B **27** (1983) 7330.
- [3] S. Doniach and M. Šunjić, J. Phys. C **3** (1970) 285.
- [4] T. Toliński, A. Kowalczyk, G. Chełkowska, Phys. Lett. A **308** (2003) 75.
- [5] T. Toliński, A. Kowalczyk, M. Pugaczowa-Michalska, G. Chełkowska, J. Phys.: Condens. Matter **15** (2003) 1397.



MAGNETISM AND ELECTRONIC STRUCTURE OF GdMnGe

B. Tyszka^a, J. Szade^a, J. Deniszczyk^b

^a*A. Chelkowski Inst. of Physics, Univ. of Silesia, Uniwersytecka 4, 40-007 Katowice, Poland*

^b*Inst. of Phys. and Chem. of Metals, Univ. of Silesia, Bankowa 12, 40-007 Katowice, Poland*

Rare-earth-transition metal germanides have been intensively studied in recent years because of the variety of interesting magnetic and crystallographic properties.

GdTiGe and compounds obtained by Mn substitution of Ti (up to 60 % at.) show ferromagnetic behaviour with T_C in the temperature range 374 K – 430 K [1]. The electronic structure of GdTiGe determined from photoemission spectra appeared to be in good agreement with the TB-LMTO calculations [2]. Among the known RTX system only the Mn compounds have essential magnetic moments in the 3d sublattice [3].

GdMnGe crystallizes in the orthorhombic TiNiSi type of structure (Pnma) ($a=7.14$, $b=4.17$, $c=8.20$ Å). The Néel temperature of 490 K has been reported by Klosek et al. [4] whereas we have found two additional transitions of the antiferromagnetic like character at 337 and 102 K. The antiferromagnetic character of ordering is confirmed by the magnetic field dependence of magnetization obtained at 1.9 K.

The nearest Mn-Mn distance has been found to be a factor determining the magnetic moment and coupling. For $d_{Mn-Mn} > 2.89$ Å an antiferromagnetic coupling has been found, whereas for lower distances ferromagnetic or mixed interaction have been reported [1]. The antiferromagnetic coupling within the Mn sublattice is in agreement with the shortest Mn-Mn distance within the TiNiSi-type of structure (3.147 Å).

Calculations using the TB-LMTO method have shown that Mn and Gd d bands are strongly polarized what leads to the Mn moment of about $3.22 \mu_B$. Antiparallel polarization of Gd and Mn d states has been found. It leads to the ferrimagnetic character of magnetic ordering in GdMnGe.

[1] B. Tyszka, J. Szade, J. Alloys Comp., in press

[2] G. Skorek, J. Deniszczyk, J. Szade, B. Tyszka, J. Phys.: Cond. Matter 13 (2000) 6397

[3] A. Szytuła, Crystal Structure and Magnetic Properties of RTX Rare Earth Intermetallics, Jagiellonian University, Cracow, 1998

[4] V. Klosek, A. Verniere, B. Ouladdiaf, B. Malaman, J. Magn. Magn. Mater. 256 (2003) 69



LIST OF PARTICIPANTS

K. Baberschke

Freie Universitaet Berlin
Institut fuer Experimentalphysik
Arnimallee 14
D 14195 BERLIN-Dahlem, Germany
phone: +49-30-8385-2648 (fax -3646)
Email: bab@physik.fu-berlin.de
<http://www.physik.fu-berlin.de/~ag-baberschke/index.html>

M. Bąk

Institute of Physics, A. Mickiewicz University,
ul. Umultowska 85,
61-614 Poznań, Poland
Email: karen@amu.edu.pl

J. Baszyński

Institute of Molecular Physics,
Polish Academy of Sciences,
ul. M. Smoluchowskiego 17,
60-179 Poznań, Poland
Phone: +48 61 8695 100
Fax: +48 61 8684 524
Email: Janusz.Baszynski@ifmpan.poznan.pl

S. Bluegel

IFF, Forschungszentrum Juelich,
D-52425 Juelich, Germany
Email: S.Bluegel@fz-juelich.de

G. Chelkowska

Department of Physics,
Silesian University,
Uniwersytecka 4,
40-007 Katowice, Poland
Email: gchelkow@us.edu.pl

J. Deniszczyk

Institute of Physics and Chemistry of Metals,
University of Silesia,
Bankowa 12, 40-007 Katowice, Poland
Phone: +48 32 3591418
E-mail: jdeni@us.edu.pl



E. Długaszewska

Institute of Molecular Physics,
Polish Academy of Sciences,
ul. M. Smoluchowskiego 17,
60-179 Poznań, Poland
Phone: +48 61 8695 100
Fax: +48 61 8684 524
Email: ewa@ifmpan.poznan.pl

J. Dubowik

Institute of Molecular Physics,
Polish Academy of Sciences,
ul. M. Smoluchowskiego 17,
60-179 Poznań, Poland
Phone: +48 61 8695 100
Fax: +48 61 8684 524
Email: Janusz.Dubowik@ifmpan.poznan.pl

K. Dziatkowski

Faculty of Physics, Warsaw University, Hoża 69
00-681 Warszawa, Poland
Phone: +48225532194
Fax: +48226219712
E-mail: Konrad.Dziatkowski@fuw.edu.pl

H. Ebert

Ludwig-Maximilians-Universitaet Muenchen
Department Chemie
Physikalische Chemie
Butenandtstrasse 11
Haus E, Raum 2.033
D-81377 Muenchen
Tel.: +49 89 2180-77583
Fax.: +49 89 2180-77584
Email: Hubert.Ebert@cup.uni-muenchen.de

O. Eriksson

Uppsala University
Department of Physics,
Theoretical Magnetism Group,
Box 530, SE-751 21 Uppsala, Sweden.
Tel: +46 (0)18 471 3625
Email: Olle.Eriksson@fysik.uu.se



H. Eschrig

IFW Dresden,
P.O.Box 27 00 16,
D-01171 Dresden, Germany
Tel. +49 (351) 4659 380
Fax. +49 (351) 4659 500
Email: h.eschrig@ifw-dresden.de

V. Eyert

Universitaet Augsburg, Augsburg, Germany
Institut fuer Physik, Universitaet Augsburg
UniversitaetsstraÙe 1,
86135 Augsburg, Germany
phone: +49-821-598-3240
fax: +49-821-598-3262
Email: eyert@physik.uni-augsburg.de

J.E. Frackowiak

Institute of Physics and Chemistry of Metals,
University of Silesia,
Bankowa 12,
40-007 Katowice, Poland
Phone: +48 (32) 359-1117
Fax: +48 (32) 259-69-29
E-mail: jfrack@us.edu.pl

A. Go

Institute of Experimental Physics,
University of Białystok,
Lipowa 41,
15-424 Białystok, Poland
Phone: +48-85-7457249
Fax: +48-85-7457223
E-mail: annago@alpha.uwb.edu.pl

J. Goraus

Institute of Physics, University of Silesia,
Uniwersytecka 4, 40-007 Katowice, Poland
Phone: +48 32 2588431, +48 32 3591298
Fax: +48 32 2588431
E-mail: jgoraus@o2.pl

J.-M. Greneche

Laboratoire de Physique de l'Etat Condensé ,
UMR CNRS 6087 Université du Maine,
72085 Le Mans Cedex 9, France
E-mail: greneche@univ-lemans.fr



J. Hafner

Institut fuer Materialphysik
and Center for Computational Materials Science
Universitaet Wien
Sensengasse 8/12
A-1090 WIEN, Austria
Tel.: +43-1-4277-51400
FAX : +43-1-4277-9514
Email: juergen.hafner@univie.ac.at
<http://cms.mpi.univie.ac.at>

M. Haglauer

Institute of Physics,
A. Mickiewicz University,
ul. Umultowska 85,
61-614 Poznań, Poland

B. Idzikowski

Institute of Molecular Physics,
Polish Academy of Sciences,
ul. M. Smoluchowskiego 17,
60-179 Poznań, Poland
Phone: +48 61 8695 100
Fax: +48 61 8684 524
Email: idzi@ifmpan.poznan.pl

H.S. Jeevan

Max-Planck-Institute for Chemical Physics of Solids,
Nothnitzer Str. 40,
D-01187 Dresden, Germany
Phone: +49-351-4646-2249
Fax: +49-351-4646-2262
E-mail: jeevan@cpfs.mpg.de

A. Jezierski

Institute of Molecular Physics,
Polish Academy of Sciences,
ul. M. Smoluchowskiego 17,
60-179 Poznań, Poland
Phone: +48 61 8695 100
Fax: +48 61 8684 524
Email: Andrzej.Jezierski@ifmpan.poznan.pl



T. Jungwirth

Department of Surfaces and Interfaces
Institute of Physics
Academy of Sciences of the Czech Republic
Cukrovarnicka 10
Prague 6, Czech Republic 162 53
Office phone: 420-2-20318457
Fax: 420-2-33343184
Email: jungw@fzu.cz

M. Jurczyk

Institute of Materials Science and Engineering,
Poznan University of Technology,
Skłodowska-Curie 5 Sq., 60-695 Poznan, Poland
Email: mieczyslaw.jurczyk@put.poznan.pl

J. Kirschner

Max-Planck Institut fuer Mikrostrukturphysik,
Weinberg 2,
D-06120 Halle, Germany
Email: sekrki@mpi-halle.mpg.de

M. Košuth

Ludwig-Maximilians-University Muenichen
Department Chemistry/ Physical Chemistry
Butenandtstrasse 11
House E, Room 2.033
81377 Muenichen
GERMANY
Tel.: +49 89 2180-77577
Fax.: +49 89 2180-77568
Email: Michal.Kosuth@cup.uni-muenchen.de

A. Kowalczyk

Institute of Molecular Physics,
Polish Academy of Sciences,
ul. M. Smoluchowskiego 17,
60-179 Poznań, Poland
Fax: +48 61 8684 524
Phone: +48 61 8695 100
Email: ankow@ifmpan.poznan.pl

M. Krawczyk

Surface Physics Division, Faculty of Physics,
A. Mickiewicz University,
ul. Umultowska 85,
61-614 Poznan, Poland;



S. Krompiewski

Institute of Molecular Physics,
Polish Academy of Sciences,
ul. M. Smoluchowskiego 17,
60-179 Poznań, Poland
Phone: +48 61 8695 100
Fax: +48 61 8684 524
Email: stefan@ifmpan.poznan.pl

H. Kroha

Physikalisches Institut der
Universitaet Bonn
Nussallee 12
D-53115 Bonn, Germany
Phone: ++49-228-73-2798
Fax: ++49-228-73-3223
E-mail: kroha@th.physik.uni-bonn.de
WWW: <http://www.th.physik.uni-bonn.de/th/Groups/Kroha>

M. Leżaić

Forschungszentrum Juelich
IFF, Forschungszentrum Juelich
D-52425 Juelich, Germany
Phone: +49 2461 61 4627
Fax: +49 2461 61 2620
E-mail: m.lezaic@fz-juelich.de

H. von Loehneysen

Forschungszentrum Karlsruhe
Institut fuer Festkoerperphysik
Postfach 3640
D-76021 Karlsruhe, Germany
Fax: 07247-82-4624
Email: h.vL@ifp.fzk.de

T. Luciński

Institute of Molecular Physics,
Polish Academy of Sciences,
ul. M. Smoluchowskiego 17,
60-179 Poznań, Poland
Phone: +48 61 8695 100
Fax: +48 61 8684 524
Email: Tadeusz.Lucinski@ifmpan.poznan.pl



S. Mamica

Surface Physics Division,
Faculty of Physics,
A. Mickiewicz University,
ul. Umultowska 85,
61-614 Poznań, Poland
phone: (+48-61) 829 5059
fax: (+48-61) 825 7758
Email: mamica@main.amu.edu.pl

Ph. Mavropoulos

Forschungszentrum Juelich
IFF, Forschungszentrum Juelich
D-52425 Juelich, Germany
Phone: +49 2461 61 5956
Fax: +49 2461 61 2620
E-mail: ph.mavropoulos@fz-juelich.de

T. Michalecki

Institute of Physics and Chemistry of Metals,
University of Silesia,
Bankowa 12,
40-007 Katowice, Poland
Phone: +48 32 3591776
E-mail: tomek@beta.ifichm.us.edu.pl

G. Michalek

Institute of Molecular Physics,
Polish Academy of Sciences,
ul. M. Smoluchowskiego 17,
60-179 Poznań, Poland
Phone: +48 61 8695 100
Fax: +48 61 8684 524
Email: Grzegorz.Michalek@ifmpan.poznan.pl

J.A. Morkowski

Institute of Molecular Physics,
Polish Academy of Sciences,
ul. M. Smoluchowskiego 17,
60-179 Poznań, Poland
Phone: +48 61 8695 100
Fax: +48 61 8684 524
Email: Janusz.Morkowski@ifmpan.poznan.pl



K.-H. Mueller

IFW Dresden,
P.O.Box 27 00 16,
D-01171 Dresden, Germany
Email: K.H.Mueller@ifw-dresden.de

P. Napierala

Institute of Molecular Physics,
Polish Academy of Sciences,
ul. M. Smoluchowskiego 17,
60-179 Poznań, Poland
Phone: +48 61 8695 100
Fax: +48 61 8684 524
Email: Piotr.Napierala@ifmpan.poznan.pl

M. Nogala

Institute of Physics, A. Mickiewicz University,
ul. Umultowska 85,
61-614 Poznań, Poland

L. Nordstroem

Uppsala University
Department of Physics,
Theoretical Magnetism Group,
Box 530, SE-751 21 Uppsala, Sweden.
Tel:+46-(0)18 471 7309
Email: Lars.Nordstrom@fysik.uu.se

F. Petroff

Chargé de Recherche au CNRS
Unité Mixte de Physique
CNRS/THALES (CNRS-UMR137)
Domaine de Corbeville,
91404 Orsay, France
tel +33 (0)1 69 33 90 65
fax +33 (0)1 69 33 07 40
E-mail : frederic.petroff@thalesgroup.com
<http://www.lcr.thomson-csf.com/cnrs/umr137.html>

A. Postnikov

Universitaet Osnabrueck
Fachbereich Physik,
D-49069 Osnabrueck, Germany
Tel. +49-541-969.2377 -- Fax .2351
Email: apostnik@uos.de
<http://www.home.uni-osnabrueck.de/apostnik/>



H. Puzkarski

Surface Physics Division,
Faculty of Physics, A. Mickiewicz University,
ul. Umultowska 85,
61-614 Poznań, Poland

M. Przybylski

Max-Planck-Institut fuer Mikrostrukturphysik
Weinberg 2
D-06120 Halle, Germany
Phone: +49 345 5582 969
Fax: +49 345 5511223
E-mail: mprzybyl@mpi-halle.de

M. Pugaczowa-Michalska

Institute of Molecular Physics,
Polish Academy of Sciences,
ul. M. Smoluchowskiego 17,
60-179 Poznań, Poland
Fax: +48 61 8684 524
Email: maria@ifmpan.poznan.pl

K. Rećko

Institute of Experimental Physics,
University of Białystok,
ul. Lipowa 41,
15-424 Białystok, Poland
Phone: +48-85 745 72 46
Fax: +48-85 745 72 23
E-mail: karo@alpha.uwb.edu.pl

M. Richter

Dept. of Theoretical Solid State Physics
IFW Dresden e.V.
P.O. Box 270016
D-01171 Dresden, Germany
Tel. +49-351-4659-360
Fax. +49-351-4659-490
email m.richter@ifw-dresden.de
www <http://www.ifw-dresden.de/~manuel>

A. Ślebarski

Department of Physics,
Silesian University,
Uniwersytecka 4,
40-007 Katowice, Poland
Email: slebar@us.edu.pl



Centre of Excellence: Magnetic and Molecular Materials for Future Electronics

Institute of Molecular Physics, Polish Academy of Sciences
ul. Mariana Smoluchowskiego 17, 60-179 Poznań, Poland

L. Smardz

Institute of Molecular Physics,
Polish Academy of Sciences,
ul. M. Smoluchowskiego 17,
60-179 Poznań, Poland
Phone: +48 61 8695 100
Fax: +48 61 8684 524
Email: smardz@ifmpan.poznan.pl

P. Stefański

Institute of Molecular Physics,
Polish Academy of Sciences,
ul. M. Smoluchowskiego 17,
60-179 Poznań, Poland
Phone: +48 61 8695 100
Fax: +48 61 8684 524
Email: Piotr.Stefanski@ifmpan.poznan.pl

F. Stobiecki

Institute of Molecular Physics,
Polish Academy of Sciences,
ul. M. Smoluchowskiego 17,
60-179 Poznań, Poland
Phone: +48 61 8695 100
Fax: +48 61 8684 524
Email: Feliks.Stobiecki@ifmpan.poznan.pl

A. Szajek

Institute of Molecular Physics,
Polish Academy of Sciences,
ul. M. Smoluchowskiego 17,
60-179 Poznań, Poland
Phone: +48 61 8695 100
Fax: +48 61 8684 524
Email: szajek@ifmpan.poznan.pl

A. Szlaferek

Institute of Molecular Physics,
Polish Academy of Sciences,
ul. M. Smoluchowskiego 17,
60-179 Poznań, Poland
Phone: +48 61 8695 100
Fax: +48 61 8684 524
Email: Andrzej.Szlaferek@ifmpan.poznan.pl



Z. Szotek

Daresbury Laboratory, Daresbury,
Warrington, Cheshire WA4 4AD
U.K.
+44 1925 603227
+44 1925 603634
Email: z.szotek@dl.ac.uk

W. Temmerman

Daresbury Laboratory, Daresbury,
Warrington, Cheshire WA4 4AD
U.K.
+44 1925 603227
+44 1925 603634
Email: w.m.temmerman@dl.ac.uk

T. Toliński

Freie Universitaet Berlin
Institut fuer Experimentalphysik
Arnimallee 14
D-14195 BERLIN-Dahlem, Germany
Email: tomtol@ifmpan.poznan.pl
babgroup@physik.fu-berlin.de

B. Tyszka

A. Chelkowski Institute of Physics,
University of Silesia
Uniwersytecka 4,
40-007 Katowice, Poland
Phone: +48 323591740
Fax: +48 32 2588431
E-mail: beata@kulpa.zfcst.us.edu.pl

R. Wiesendanger

Institute of Applied Physics (IAP)
Microstructure Advanced Research Center Hamburg (MARCH)
German Center of Competence in Nano-Scale Analysis (CCN)
Interdisciplinary Nanoscience Center Hamburg (INCH)
University of Hamburg, Jungiusstrasse 11
D-20355 Hamburg, Germany
Tel.: *49-40-42838-5244, FAX: *49-40-42838-6188
Email: wiesendanger@physnet.uni-hamburg.de
<http://www.nanoscience.de>
<http://www.nanoscience.de/hansenanonet>
<http://www.nanoanalytik-hamburg.de>
<http://www.nanotechnologie-eV.de>



T. Zawada

Institute of Physics,
University of Silesia,
Uniwersytecka 4,
40-007 Katowice, Poland
Phone: +48 32 2588 431
Fax: +48 32 2588 431
E-mail: tomekz@polbox.com

M. Zwierzycki

Computational Materials Science
Faculty of Applied Physics
University of Twente
P.O. Box 217
7500 AE Enschede
The Netherlands
Tel. +31-53-4891082
Fax: +31-53-4892910
Email: M.Zwierzycki@utwente.nl



Centre of Excellence: Magnetic and Molecular Materials for Future Electronics

**Institute of Molecular Physics, Polish Academy of Sciences
ul. Mariana Smoluchowskiego 17, 60-179 Poznań, Poland**

INDEX OF NAMES

- | | | |
|--------------------------|-------------------------------|----------------------------|
| B. Andrzejewski 45, 64 | E. Kosubek 62 | A. Svane 20, 21 |
| K. Baberschke 2, 62 | M. Košuth 27 | J. Szade 68 |
| G.E.W. Bauer 36 | B.Yu. Kotur 53 | A. Szajek 26, 59 |
| G. Bihlmayer 3, 44 | A. Kowalczyk 52, 64, 66 | A. Szlaferek 60, 64, 66 |
| S. Bluegel 3, 44 | M. Krawczyk 48 | Z. Szotek 20, 21 |
| B.R. Bułka 57 | H. Kroha 13 | B. Szymański 34 |
| A. Caramico D'Auria 41 | S. Krompiewski 28 | K. Szymański 53 |
| G. Chełkowska 52, 64, 66 | A. Kumar 12 | A. Ślebarski 19 |
| P.H. Dederichs 49 | K. Lenz 62 | M. Talanana 36 |
| J. Deniszczyk 37, 50, 68 | J.-C.S. Lévy 48 | W.M. Temmerman 20, 21 |
| M. Deppe 42 | M. Leżaić 44 | T. Toliński 52, 62, 64, 66 |
| H.F. Ding 12 | J. Lindner 62 | B. Tyszka 68 |
| L. Dobrzyński 39, 53 | H. von Loehneysen 14 | M. Urbaniak 34, 45 |
| J. Dubowik 25, 34 | T. Luciński 34, 45 | R. Vollmer 12 |
| H. Ebert 4, 27 | M. Lueders 21 | P. Wandziuk 45 |
| O. Eriksson 5 | S. Mamica 47, 48 | R. Wiesendanger 22 |
| A. Ernst 21 | Ph. Mavropoulos 49 | H. Winter 20, 21 |
| H. Eschrig 6 | T. Michalecki 50 | D. Wortmann 3 |
| F. Esposito 41 | J.A. Morkowski 29 | W. Wulfhekel 12 |
| M. Etzkorn 12 | K.-H. Mueller 15 | K. Xia 36 |
| V. Eyert 7 | P. Napierała 43 | M. Zwierzycki 36 |
| M. Falkowski 66 | L. Nordstroem 17 | |
| E. Faulhaber 42 | M. Nowak 55 | |
| J.E. Fraćkowiak 37, 50 | I. Ophale 6 | |
| I. Galanakis 49 | A. Paetzold 25 | |
| C. Geibel 42 | L. Petit 20, 21 | |
| A. Go 39 | F. Petroff 18 | |
| I. Gościańska 25 | V. Popescu 27 | |
| J.-M. Greneche 8, 26 | A. Postnikov 30 | |
| J. Hafner 9, 10 | M. Przybylski 32 | |
| M. Haglauer 41 | M. Pugaczowa-Michalska 39, 52 | |
| B.C. Hauback 53 | H. Puzkarski 47, 48 | |
| S. Heinze 3 | K. Rećko 53 | |
| W. Hergert 20 | M. Richter 6, 33 | |
| A. Hoser 64 | K. Roell 25, 34 | |
| H. Ibach 12 | D. Satuła 53 | |
| B. Idzikowski 26 | W. Schaefer 64 | |
| V. Ivanov 66 | U. Schlickum 12 | |
| H.S. Jeevan 42 | K. Smardz 55 | |
| A. Jezierski 19, 43 | L. Smardz 55 | |
| T. Jungwirth 11 | D. Spisak 9, 10 | |
| M. Jurczyk 55 | P. Stefański 57 | |
| G. Kamieniarz 41 | F. Stobiecki 34 | |
| P.J. Kelly 36 | O. Stockert 42 | |
| J. Kirschner 12 | G.M. Stocks 20 | |
| W. Kockelmann 64 | P. Strange 21 | |
| D. Koedderitzsch 20, 21 | W. Suski 53 | |

